PALEOCEANOGRAPHY, VOL. 28, 539–561, doi:10.1002/palo.20046, 2013

The role of deep ocean circulation in setting glacial climates

Jess F. Adkins [1]

Received 2 January 2013; revised 1 August 2013; accepted 16 August 2013; published 19 September 2013.

[1] The glacial cycles of the Pleistocene involve changes in the circulation of the deep ocean in important ways. This review seeks to establish what were the robust patterns of deep-sea water mass changes and how they might have influenced important parts of the last glacial cycle. After a brief review of how tracers in the modern ocean can be used to understand the distribution of water masses, I examine the data for biogeochemical, circulation rate, and conservative tracers during glacial climates. Some of the robust results from the literature of the last 30 years include: a shoaled version of northern source deep water in the Atlantic, expanded southern source water in the abyss and deep ocean, salt (rather than heat) stratification of the last glacial maximum (LGM) deep-sea, and several lines of evidence for slower overturning circulation in the southern deep cell. We combine these observations into a new idea for how the ocean-atmosphere system moves from interglacial to glacial periods across a single cycle. By virtue of its influence on the melting of land-based ice around Antarctica, cooling North Atlantic Deep Water (NADW) leads to a cold and salty version of Antarctic Bottom Water (AABW). This previously underappreciated feedback can lead to a more stratified deep ocean that operates as a more effective carbon trap than the modern, helping to lower atmospheric CO_2 and providing a mechanism for the deep ocean to synchronize the hemispheres in a positive feedback that drives the system to further cooling.

Citation: Adkins, J. F. (2013), The role of deep ocean circulation in setting glacial climates, *Paleoceanography*, *28*, 539–561, doi:10.1002/palo.20046.

1. Introduction

[2] The role of the deep ocean in climate change has been a central theme of paleoceanography from the early days of the field. As the locus of nearly all the mass, thermal inertia, and carbon in the ocean-atmosphere system, the deep ocean's behavior is an important parameter in understanding past climates—whether considering either the steady states or the propensity for rapid shifts. There are two observations from ice cores that particularly motivate the investigation of past deep ocean circulation in the context of past climate change. One of these is the carbon cycle changes demanded by the past atmospheric CO_2 data from Antarctica, which show significant variability across glacial to interglacial cycles [*Barnola et al*., 1987; *Neftel et al*., 1985]. In these records, air temperature and CO_2 closely follow each other over the last 850,000 years [*EPICA*, 2004]. However, at glacial terminations, there is a strong nonlinearity in each of these variables relative to the proposed insolation forcing during boreal summers (Figure 1). The classic "sawtooth" structure of glacial cycles [*Broecker and van Donk*, 1970] is punctuated by rapid increases in sea level, temperature, and CO_2 that require a nonlinear response of the ocean-atmosphere system to solar forcing. While CO_2 does not seem to initiate deglaciations [*Caillon et al*., 2003], its role as a greenhouse gas is one of the most important amplifiers to temperature change during these climate transitions. Because of the acid dissociation constants of the carbonate system and the alkalinity content of the ocean—today there is 60 times more carbon in the deep ocean than in the atmosphere—any past changes in atmospheric CO_2 must involve the carbon dynamics of the deep ocean reservoir.

[3] The quantitative role that the deep ocean circulation plays in the lowering of glacial pCO_2 has been an important area of research since the mid-1980s. With the publication of the so-called "Harvardton Bears" box models [*Knox and McElroy*, 1984; *Sarmiento and Toggweiler*, 1984; *Siegenthaler and Wenk*, 1984], the joint dependence of the system on deep ocean ventilation rates and high latitude biological productivity became clear (Figure 2). These simple models pointed out that the Southern Ocean is the atmospheric window to the large volumes of the deep ocean; thus, the processes in this region must mediate the storage of carbon in the deep ocean (and its removal from the atmosphere during the glacial periods). Toggweiler [*Toggweiler*, 1999] expanded on this work by building a series of box models that moved the deep ocean upwelling from the low latitudes to the high latitudes (four boxes), emphasized the importance of intermediate waters (six boxes), and divided the deep box into two regions ventilated from the south and the north separately (seven boxes) (Figure 2a). The paleo data were better explained with each of these sequential enhancements to the simplest box models, but the basic implication that both productivity changes and deep ocean circulation rate changes are necessary to produce significant atmospheric CO_2 change is clearly consistent across models, regardless of configuration Figure 2b.

[1]Division of Geology and Planetary Sciences Caltech, Pasadena, California, USA.

Corresponding author: J. F. Adkins, Division of Geology and Planetary Sciences, MS 131-24, Caltech, Pasadena, CA 91125, USA. (jess@gps.caltech.edu)

0883-8305/13/10.1002/palo.20046

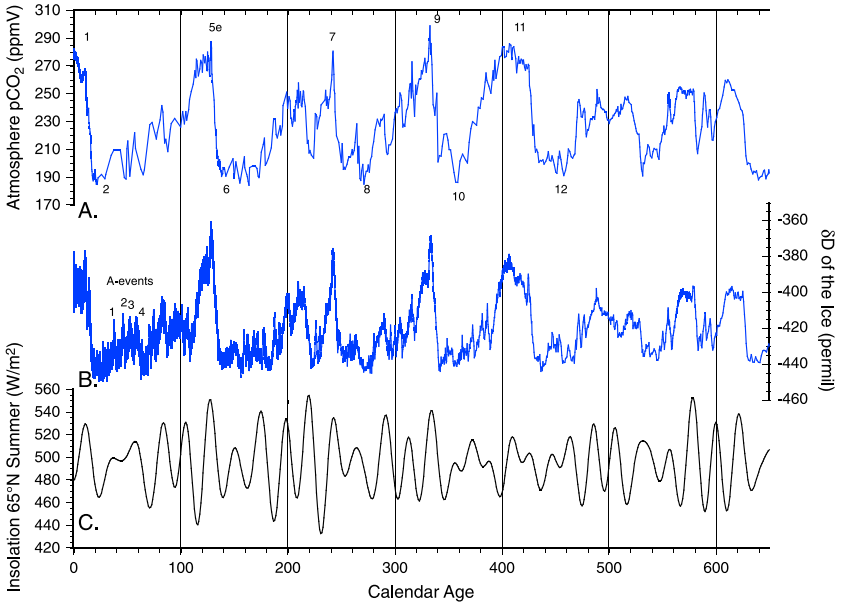

Figure 1. Ice core records of (a) pCO_2 and (b) δD of the ice along with summer solar insolation at 65°N (c). Marine Isotope Stages are labeled in Figure 1A. and Antarctic "A-events" are labeled in Figure 1B. The "saw-tooth" character of the ice core temperature proxy δD has a strong 100 ka signal that is not easily seen in the insolation forcing curve. Carbon dioxide can work as an amplifier of insolation forcing during terminations and might provide the "kick" for rapid deglacial warmings. If CO_2 matters in the glacial-interglacial climate system, then the deep ocean nutrient and circulation dynamics must play a role in these climate changes.

[4] But changing pCO_2 is the not the only motivation for examining changes in the deep circulation through glacial cycles. Over the last 20 years, studies of past climate have undergone a profound change in emphasis from a glacial-interglacial approach to the study of rapid shifts in the system. By cross correlating isotopic records of atmospheric temperature in ice cores drilled at Greenland's summit, we now recognize the global prevalence of large amplitude climate shifts on very short time scales [*Dansgaard et al.*, 1993; *GRIP*, 1993; *Grootes et al.*, 1993; *Steffensen et al.*, 2008]. What were formerly considered uncorrelated wiggles in the Greenland archives are now well established to be real climate signal [*Alley et al.*, 1995]. While Milankovitch cycles are the fundamental pacemakers of climate at 20, 40, and 100 thousand year periods, research emphasis has switched to the observations of much more rapid fluctuations at the centennial to decadal timescale. Twenty-two separate interstadial events—brief returns to warmer climate—have been recognized in the Greenland

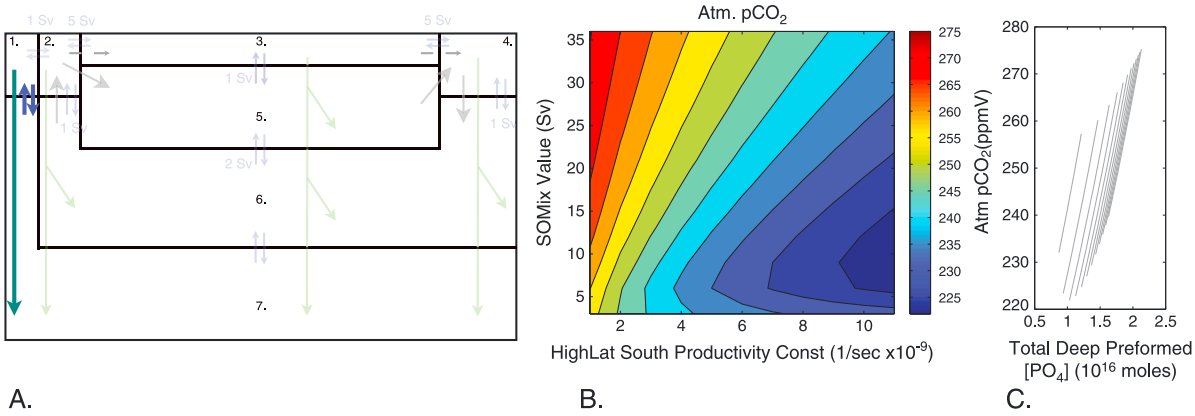

Figure 2. Sensitivity of pCO_2 to changes in biological production and deep-ocean overturning rate as calculated in a multibox model [after *Toggweiler*, 1999]. It is not possible to move from preindustrial values of ~280 ppmV to LGM values of 180–200 ppmV without changing both the biology of the Southern Ocean (bold green arrow) and the deep ocean overturning strength (bold blue arrows). While there are several caveats to these model results discussed in the text and examined in detail in *Hain et al.* [2011], results for a single productivity constant and varying the Southern Ocean overturning show a simple dependence of pCO_2 on the integrated amount of preformed phosphate ion in the deep ocean [after *Sigman et al.*, 2010]. A full description of the model shown here will appear in a future paper.

summit ice core records. Large volumes of ice rafted debris are recognized roughly every 7000 years in North Atlantic sediments as armadas of icebergs were shed from continental ice sheets in so-called "Heinrich Events" [*Heinrich*, 1988; *Hemming*, 2004; *Ruddiman et al*., 1980]. And the data are not limited to the North Atlantic, with Greenland-like variation in the Santa Barbara Basin [*Behl and Kennett*, 1996], the Southern Ocean [*Charles et al*., 1996], the Indian Ocean [*Schulz et al*., 1998], and the Chinese Monsoon [*Wang et al*., 2001]. Collectively these observations represent a challenge for paleoclimate studies. One of the largest outstanding questions in our field is the issue of what mechanisms cause these large and rapid shifts (Heinrich, deglacial, and interstadial) and, more specifically, what is the role of deep ocean circulation in their realization [*Boyle*, 2000]?

[5] Broecker introduced the notion of a "salt-oscillator" in the North Atlantic to explain both the rapid shifts and the glacial-interglacial differences seen in paleo records. He hypothesized that North Atlantic Deep Water (NADW) was close to an instability threshold with respect to salinity. In this early idea, the opposing forces of fresh water export out of the Atlantic basin over Central America via the atmosphere and salt export via NADW transport out of the basin lead to oscillations in the climate system. While NADW formation is active, its associated cooling of the ocean warms the atmosphere and greatly alters the heat budget of the North Atlantic. Coupling this fresh water balance to the observation of phasing between Greenland and Antarctic ice cores resulted in a modified salt-oscillator idea, the "bipolar seesaw" [*Broecker*, 1998; *Stocker*, 1998]. In its simplest form, this idea relies on radiation that has warmed the southern Atlantic to cross the equator and be released to the atmosphere as NADW sinks. In this way, a warm mode in the North Atlantic leads to a cooling of the Southern Hemisphere, an idea first put forward by Crowley [*Crowley*, 1992].

[6] Most, but not all [*Gildor and Tziperman*, 2003; *Timmerman et al*., 2003], of the current theories for why there are ice ages and/or rapid climate changes within glacial stages rely on variations in the overturning rate of the deep ocean, though the exact mechanisms at work are not yet understood and they tend to focus on NADW on or off modes. From the methane synchronization in ice cores [*Blunier and Brook*, 2001], it is clear that temperature increases in Antarctica associated with the North Atlantic Heinrich Events (so-called "A events") preceded the rapid warmings seen in Greenland by 1–3000 years. A time difference this large is not the same mechanism as the classic "see-saw" described above and must originate from a piece of the climate system with large inertia. Only the cryosphere itself and the deep ocean are large enough reservoirs to cause this very long time constant [*Imbrie et al*., 1992].

[7] With these primary motivations in mind, I will review what we do know about changes in the deep ocean circulation from paleo-tracer data. The paper is not a review of mechanisms for glacial to interglacial CO_2 change [*Sigman and Boyle*, 2000; *Sigman et al*., 2010] or a review of proposed mechanisms for rapid climate change. Instead, I hope to show what data are available from the interior of the ocean and how we might quantify them, with an emphasis on the last glacial maximum (LGM). The paper does not start from the same place as an inverse approach with the question "what was the past circulation, and can I establish within error that it was different than today" [*LeGrand and Wunsch*, 1995]. Instead, I think from the above discussion, it is clear that the deep sea has a crucial role to play in past climate changes, and, accordingly, it is essential to review what it is we can extract from the tracer information to better understand this role. The question of what drives changes in the deep ocean circulation is a fascinating and open research topic in modern oceanography and one where paleoclimate studies could help provide an answer in the future. However, the motivation for understanding the rate of deep ocean ventilation is not necessarily to reconstruct the full circulation. For example, the pCO_2 changes require an understanding of how ocean carbon and alkalinity are transported and diffused in the fluid, just like any tracer affected by circulation. To this end, I will also review a relatively new method of using tracer balances to constrain important parameters of the past circulation after summarizing what we know about the tracer distributions themselves. At the end, I will propose a new idea for how the LGM circulation pattern might have come about and what role it played in glacial to interglacial climate change.

2. Modern Deep Ocean Circulation

[8] There are many good reviews on the modern distribution of deep water masses and their dynamics [*Reid*, 1981; *Rintoul et al*., 2001; *Talley et al*., 2011; *Warren*, 1981], but it is instructive to consider how modern tracer information can be used in a simple way to infer deep ocean processes. Many modern studies diagnose the fluxes of heat and moisture at the ocean's surface to constrain the volumes and rates of deep water mass circulation [*Speer and Tziperman*, 1992]. As temperature and salinity are conservative tracers in the ocean interior, their rates of change at water mass outcrop regions are useful diagnostics. In paleoceanography, on the other hand, we rarely have access to these surface fluxes, but we do have information about tracers in the ocean interior. To this end, a tracer view of deep circulation begins with the distribution of salinity and potential temperature (theta). As the off axis geothermal heat flux is ~100 mW/m^2, the assumption of conservative behavior is not strictly true for potential temperature [*Emile-Geay and Madec*, 2009; *Joyce et al*., 1986], but the changes induced by bottom heating in the modern ocean are small. Sections of temperature and salinity in the Atlantic Ocean (Figures 3a and 3b) show the classic interleaving of warm/salty North Atlantic Deep Water (NADW) and cold/fresh Antarctic Bottom Water (AABW). NADW appears to "split" the southern source waters into AABW and its slightly warmer and fresher counterpart Antarctic Intermediate Water (AAIW).

[9] Because the effects of temperature and salinity on seawater density oppose each other in the two dominant deep ocean water masses, there is a class of isopycnals in the Atlantic that outcrop in both the northern and southern source water formation regions (Figure 3d). At the surface, NADW is denser than AABW due to its higher salinity. But because of the pressure dependence of the thermal expansion coefficient, the warmth of NADW makes it less dense than AABW at depth. This feature of the thermodynamics of seawater results in the fact that some isopycnal surfaces can be characterized by both nearly pure NADW and nearly pure AABW. This is true even when comparing neutral density surfaces instead of isopycnals [*Jackett and McDougall*, 1997]. Gradients in these

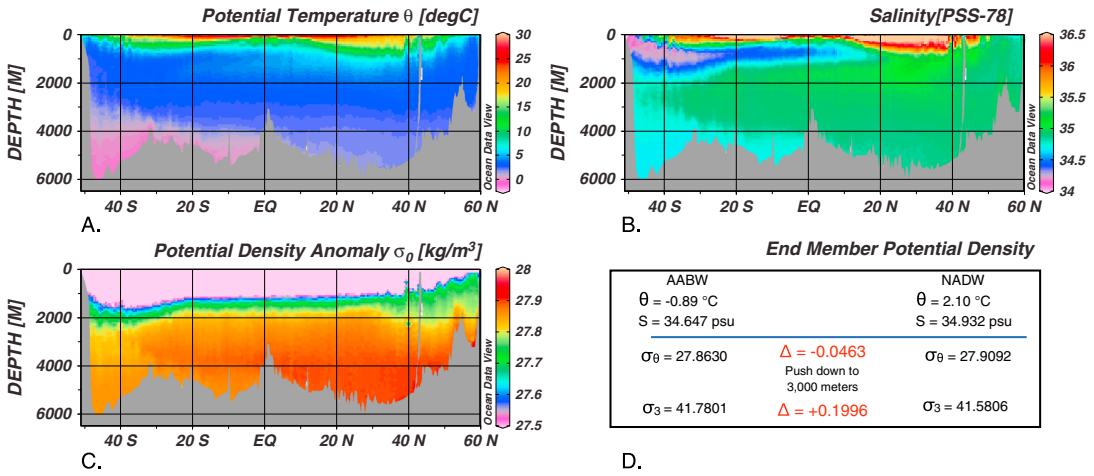

Figure 3. Sections of conservative tracers in the Western Atlantic from the GLODAP database. (a) Potential temperature, (b) salinity, (c) potential density relative to the surface pressure (σ_θ), and (D.) a calculation how σ_θ evolves for end-member T and S values of NADW and AABW. In the deep ocean, there is clear mixing between warm/salty NADW and cold/fresh AABW. The largest densities relative to the surface pressure are associated with NADW and are NOT found at the bottom of the ocean in the South Atlantic. At the surface, NADW is denser than AABW. At depth, the warmth of NADW causes it to be less dense than AABW such that this southern sourced water mass actually fills most of the abyssal ocean and much of the western basin of the South Atlantic. The change in sign of the relative densities of NADW and AABW leads to along isopycnals mixing of tracer in the modern deep Atlantic for a large volume of water.

conservative tracers along a single isopycnal give rise to a very useful diagnostic tool in modern hydrography. Plots of a conservative tracer versus a chemically active, or nonconservative, tracer like phosphate, along these dual outcropping isopycnals reveal the degree to which [PO_4] changes are due to chemical reactions or due to simple mixing of water masses with different initial [PO_4] (Figure 4b). NADW and AABW leave the surface with very different preformed phosphate values due to the large differences in the efficiency of the biological pump in the surface waters that make up each end-member. As these water masses mix together, they gain PO_4 due to the remineralization of raining organic matter from above. This process leads to deviations from a conservative mixing line in Figure 4b. At a 50/50 mixture of NADW and AABW along the 1032.1 kg/m^3 isopycnal, the chemical conversion of solid organic matter to dissolved phosphate increases the [PO_4] by ~15%.

[10] With a known remineralization rate of organic matter, and its typical phosphorous content, the deviation from conservative mixing seen in Figure 4b could be used to calculate the mean time for deep water to arrive at this site of 50/50 mixing, and thus derive circulation information from chemical tracers. Unfortunately, the integrated flux of organic matter out of the surface ocean into the deep is a difficult number to constrain in the modern, let alone the past. Radiocarbon, on the other hand, contains this rate information with no other knowledge of the system. Figure 4c plots the $\Delta^{14}C$ distribution versus potential temperature along the same isopycnal as in Figures 4a and 4b. In the Atlantic, there is about a 100‰ range in the $\Delta^{14}C$ of DIC. High salinity North Atlantic Deep Water (NADW) forms with a value of ~ −65‰ while fresher Antarctic Bottom Water (AABW) begins spreading at ~ −165‰ [*Broecker et al.*, 1995]. These numbers are somewhat uncertain because of the presence of nuclear bomb produced radiocarbon in all ocean surface waters today and the somewhat arbitrary nature of picking end-member values. Figure 4c shows that most of this 100‰ spread is due to mixing of deep water masses. Points below the pure end-member mixing line represent loss of ^{14}C due to in situ decay. The largest offset from mixing is about 30‰, corresponding to 240 ^{14}C years of isolation from the atmosphere (for this choice of two end-members). This is only a model age of the actual mass flux of water, but it is useful in the context of other tracers. Because we know the rule for nonconservative behavior of $\Delta^{14}C$ a priori—that it follows first-order radioactive decay—this tracer is much more useful than PO_4 at informing the circulation rate of the deep ocean. Radiocarbon tells us that today the Atlantic is a young ocean.

[11] These sorts of simple model ages have been replaced in modern oceanography with large data sets and sophisticated Ocean General Circulation Models (OGCMs). Both Transit Time Distributions (TTDs) [*DeVries and Primeau*, 2011; *Hall and Haine*, 2002] and inverse models attempt to use dynamical constraints on the circulation as well as tracer information to extract properties of the deep ocean. Following the pioneering work of Waugh et al. in the stratosphere [*Waugh and Hall*, 2002], the TTD approach gives rise to the notion of tracer age spectra. A single parcel contains water that arrived at that sampling site from many different pathways and many different transit times. The two end-member assumption in Figure 4 is a useful simplification, but studies of the full modern ocean suggest at least six [*Johnson*, 2008] if not many more [*Gebbie and Huybers*, 2010] end-members. Inverse models have produced flux estimates, with error bars, for deep water masses [*Ganachaud and Wunsch*, 2000] and constrained carbon export fluxes [*Schlitzer*, 2002]. The inverse approach will ultimately provide important information about the paleo deep ocean, but at the moment the tracer data set is limited enough that other approaches may produce more insight (see below).

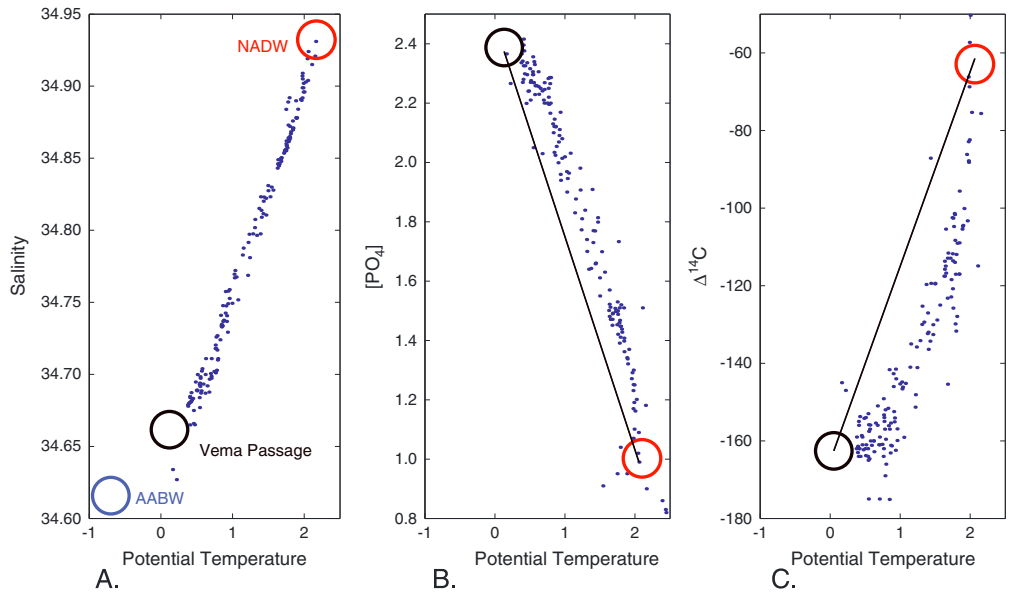

Figure 4. Tracer versus tracer plots for the deep Atlantic isopycnal $\sigma_\theta = 37.0$. (a) As both potential temperature and salinity are conservative tracers, the linear relationship implies that there are only two end-members mixing along this isopycnals at these depths. A slight offset between the "true" AABW end-member (blue circle, picked by the author) and the value at the end of the line is due to the deep mixing choke point at the Vema Passage in the South Atlantic (black circle). The NADW end-member (red circle) is at the opposite end of each line. (b) Potential temperature versus [PO_4]. Extra phosphate above the conservative mixing line comes from remineralization of raining organic matter along this isopycnal. (c) Curvature from the nonconservative $\Delta^{14}C$ versus conservative potential temperature plot arises from radioactive decay of ^{14}C along the deep isopycnal trajectory. While there is a large range of $\Delta^{14}C$ in the modern deep Atlantic, most of this variance is due to water mass mixing and NOT due to older ventilation ages. At a 50/50 mixture of NADW and AABW/Vema Passage end-members, the $\Delta^{14}C$ is ~30‰ lower than the conservative mixing line, implying about 250 years of in situ aging. Deep waters in the Western Atlantic are relatively young.

3. History

3.1. Biogeochemistry-Based Tracers

[12] One of the most robust results of deep water paleoceanography is that the mixing ratio of northern and southern source waters in the Atlantic varied on glacial-interglacial timescales. Today this result is based on a relatively large number of chemical tracer data but the first evidence came from benthic foraminifera faunal abundances. Streeter and Shackleton [*Streeter and Shackleton*, 1979] noticed that the percentage of *Uvigerina peregrina* relative to other benthic species in core V29-179 (44.7 N, 24.5 W, 3331 m) varied with the $\delta^{18}O$ isotope stages. Core top assemblages show that this species prefers waters originating from the Southern Ocean. Combining the down core and modern observations, Streeter and Shackleton concluded that "*Uvigerina* does not like NADW" and that during interglacials the retreat of *Uvigerina* in the Atlantic implies a dominance of waters from the north, but during glacial periods the *Uvigerina* compatible AABW was more dominant than it is today.

[13] Chemical tracers sensitive to the relative mixtures of Antarctic and Northern sourced waters placed this faunal-based idea in firmer context. In the early 1980s, two papers laid the foundation for much of what we think of as paleotracer oceanography today. Boyle and Keigwin [*Boyle and Keigwin*, 1982] measured Cd/Ca ratios and $\delta^{13}C$ in benthic foraminifera from the deep (~3200 m) North Atlantic and found large differences between glacial and interglacial times. Like phosphate in the modern ocean, the value of these tracers at any one location in the deep Atlantic is strongly influenced by the relative mixing ratios of northern (low Cd/Ca and high $\delta^{13}C$) and southern (high Cd/Ca and low $\delta^{13}C$) waters. Boyle and Keigwin concluded that the intensity of water mass production from the north decreased by about a factor of two as compared to deep water production from the south during severe glaciations. At nearly the same time, Curry and Lohmann [*Curry and Lohmann*, 1983] analyzed benthic $\delta^{13}C$ data from a depth transect of cores in the Eastern Equatorial Atlantic. These authors recognized that lower $\delta^{13}C$ values at depth during the LGM corresponded to a lower flux of [O_2] rich bottom waters into the Eastern Basin, as well as an increase in the overlying rain of organic matter. What these two studies have in common is a recognition that the sedimentary record could be used to reconstruct past chemical tracer information. In the same way, the modern distribution of chemical species in the deep ocean reflects ocean circulation and biogeochemistry (see above); past ocean tracer distributions can be interpreted in this framework.

[14] These studies also share the assumption that Cd/Ca and $\delta^{13}C$ in benthic foraminifera are tracers of past nutrient content of the deep waters. This interpretation is driven by the correlation in the modern ocean of low Cd/Ca and high $\delta^{13}C$ with low [PO_4] and vice versa [*Boyle*, 1988; *Kroopnick*, 1985]. For all three tracers, biological production in the surface ocean depletes the nutrient signature, and remineralization in deeper waters enriches the nutrient content. This latter process is what

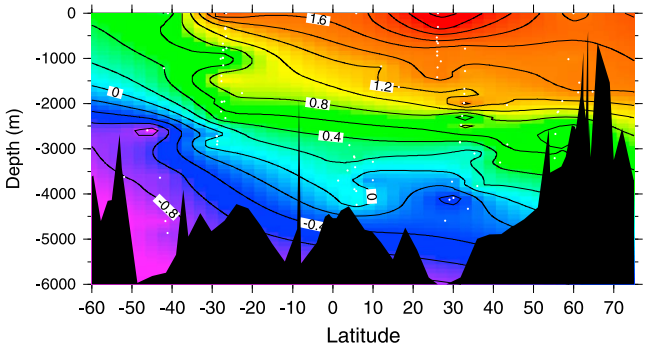

Figure 5. LGM $\delta^{13}C$ section in the Western Atlantic [after *Curry and Oppo*, 2005]. White dots are locations of data compiled and reported by Curry and Oppo. A shoaled and volumetrically more important southern sourced water mass is apparent when compared to the modern (see Figure 3). The depth transects at ~30°N and ~30°S were used in *Lund et al*. 2011a to estimate the LGM profile of the conservative property $\delta^{18}O_{CaCO3}$.

gives rise to the curvature in Figure 3b, but it is also what sets the different northern and southern end-members themselves. Modern NADW is formed from waters of subtropical origin that have been depleted of their PO_4, Cd, and ^{12}C relative to ^{13}C. Modern AABW, on the other hand, is formed from waters of higher nutrient content that experience lower overall biological nutrient utilization efficiency, thus leaving newly sinking deep waters with a higher PO_4, Cd, and ^{12}C to ^{13}C ratio. While the processes that affect these nutrient tracers are fundamentally biological, their different deep water end-member signatures provide a "quasi-conservative" tracer of the circulation.

[15] A second important assumption of this work is that the Cd/Ca ratios and $\delta^{13}C$ values recorded in benthic foraminifera are proportional to the values of the tracers in contemporaneous bottom waters. Core top calibrations of these correlations in the modern ocean are the best confirmation that this assumption is true [*Duplessy et al*., 1984]. Research into the biomineralization processes that actually set the tracer values in biogenic carbonate attempts to understand how these correlations come about [*Duplessy et al*., 1970; *Erez*, 1978; 2003]. The question, "Are foraminifera good physical chemists" is beyond the scope of this review, but the observation that modern forams produce good correlations for many different tracers is the basis for using them to constrain past circulation [*Bemis et al*., 1998; *Boyle*, 1988; *Marchal and Curry*, 2008].

[16] These early works on sedimentary tracers of paleocirculation opened the field to many new studies using both Cd/Ca and $\delta^{13}C$. Several papers emphasized that the Pacific and the Atlantic basins were always chemically distinct from one another [*Boyle and Keigwin*, 1985/6; *Shackleton et al*., 1983], though work in and around the Southern Ocean established that this glacial "end-member" looked much more like the Pacific than it does today [*Charles and Faibanks*, 1992; *Oppo and Fairbanks*, 1987]. Studies of this kind for the LGM Atlantic were compiled in a landmark paper from Duplessy et al. [*Duplessy et al*., 1988], which attempted to "map" the distribution of $\delta^{13}C$ in a north-south Western Basin section (Figure 5). This iconic figure has been redrawn several times—first by Broecker [*Broecker and Denton*, 1990] to eliminate the influence of high latitude North Atlantic planktonics, then by Sarnthein [*Sarnthein et al*., 1994] to emphasize the Eastern Basin, then by Curry and Oppo [*Curry and Oppo*, 2005] based on the addition of more South Atlantic depth transects, and finally by Marchitto and Broecker [*Marchitto and Broecker*, 2006] to depict Cd/Ca and $\delta^{13}C$ side by side. Figure 5 is modified from Curry and Oppo and shows the main features of the result. At the LGM, the deep Atlantic is filled with an isotopically depleted (nutrient-rich) water mass from the south that invades a region that is today filled by isotopically enriched (nutrient poor) northern source water. Glacial North Atlantic Intermediate Water (GNAIW) was volumetrically less important than the Glacial Southern Source Water (GSSW). This result has been interpreted many times to be the result of a reduced flux of NADW at the LGM as compared to AABW, but this interpretation ignores the importance of tracer diffusion and end-member variability in setting the values of any tracer and emphasizes the role of transport [*Marchal and Curry*, 2008; *Wunsch*, 2003]. Strategies for how one can more quantitatively extract circulation information from these tracers will be taken up in a later section.

[17] Intermediate depth records during the last deglaciation from both the North and South Atlantic show a mirror image pattern compared to time series of the abyssal water variability [*Came et al*., 2003; *Marchitto et al*., 1998; *Oppo and Horowitz*, 2000; *Rickaby and Elderfield*, 2005]. In the competition for space in the deep Atlantic between northern and southern source waters, it appears that each time the abyss is ventilated from the south (high nutrient signal) the intermediate depths see an increase in the GNAIW signature (low nutrients). Before the LGM, there is sparse coverage of deep tracer dynamics at a variety of depths, but the evidence from Marine Isotope Stage (MIS) 3 and 4 changes in deep water properties in the North Atlantic do show a strong response to Heinrich Events [*Vidal et al*., 1997]. These periods seem to be a near cessation of deep input from northern sourced water masses. There is also some evidence for D/O events in the deep ocean, with Skinner's Mg/Ca data from the North Atlantic maybe the best example [*Skinner and Elderfield*, 2007] and Charles' benthic $\delta^{13}C$ data from the South Atlantic the first to point to these changes in the deep [*Charles et al*., 1996]. Heinrich events seem to have a more robust deep water signature than the D/O transients. This feature of deep circulation is best demonstrated in cores where planktonic $\delta^{18}O$ records from the Atlantic show characteristics of one polar ice core archive,

while the benthic foraminifera records seem similar to the opposite polar ice core record Greenland ice core-like signals while the benthic stable isotopes from the same core look much more like the Antarctic record [*Charles et al*., 1996; *Curry and Oppo*, 1997; *Shackleton et al*., 2000].

[18] Other biogeochemical tracers have been developed to move beyond the mapping of paleo nutrients, mostly with the goal of understanding the ocean's role in setting pCO_2 variability. Most of these are focused on constraining pieces of the past carbon system, and while they are not strictly circulation tracers, they do respond to changes in deep water mass structure. Using Ba/Ca ratios from benthic foraminifera, Lea et al. established this deeply regenerated species as a paleo alkalinity tracer [*Lea and Boyle*, 1989; *Lea and Boyle*, 1990]. When combined with nutrient data, the record from 4200 m deep in the South Atlantic (core RC13-229 in the Cape Basin) shows inferred carbonate ion concentrations that were anticorrelated with pCO_2 over two glacial cycles [*Lea*, 1995]. Marchitto et al. have developed the combined use of Zn/Ca and Cd/Ca in benthic forams to estimate past $[CO_3]$ as well. Here the link to the carbonate system is based on the idea that Zn and Cd have different incorporation ratios into biogenic calcite at different calcite under saturation states [*Marchitto et al*., 2000]. Two aspects of boron chemistry have also been used to construct similar information. Boron isotope values in planktonic foraminifera seem to follow ambient pH in culture data [*Hönisch et al*., 2003; *Sanyal et al*., 1996] and show a glacial to interglacial signal that is consistent with the ice core pCO_2 data [*Hönisch et al*., 2009; *Sanyal et al*., 1995]. The extension of this tracer into benthic forams is a promising new advance to study deep ocean carbonate chemistry [*Rae et al*., 2011]. Recently the B/Ca ratios themselves have been implicated as a deep water saturation state tracer [*Yu and Elderfield*, 2007] and have been usefully employed to study the atmosphere and ocean carbon reservoir exchanges during the last deglaciation [*Yu et al*., 2010]. The details of these and other similar studies are easily the subject of a separate review paper of their own.

3.2. Physically Based Tracers of Water Mass Mixing Ratios

[19] Analysis of the fluxes that set the modern tracer distributions in the deep ocean is greatly aided by having both a conservative tracer, like T and S, and a nonconservative tracer, like $[PO_4]$, [Cd], or $\delta^{13}C$. As described above, in paleoceanography the nonconservative tracers can be interpreted in a "quasi-conservative" framework, but the tracer information content would be much more clear if we could make tracer-tracer plots (like those in Figure 3) with a species that only responds to the mixing of deep water masses. The combination of $\delta^{13}C$ and Cd/Ca data has been proposed as one such tracer. Recognizing that surface $\delta^{13}C$ is set by both nutrient dynamics and air-sea gas exchange, while Cd/Ca is only set by nutrient fluxes, Charles et al. [*Charles et al*., 1993] proposed that the "thermodynamic" component of $\delta^{13}C$, called $\delta^{13}C_{as}$, should be a significant fraction of the total $\delta^{13}C$ variability in surface and intermediate water DIC. In the intermediate waters south of Australia, Lynch-Stieglitz et al. combined Cd/Ca and $\delta^{13}C$ to estimate the $\delta^{13}C_{as}$ and use it as a conservative mixing tracer [*Lynch-Stieglitz et al*., 1995]. Unfortunately the data are very scattered and few studies have followed up on this tracer.

[20] The isotopes of Nd (ε_{Nd}) found in sediments [*Piotrowski et al*., 2005; *Rutberg et al*., 2000], forams [*Elmore et al*., 2011], deep-sea corals [*van der Flierdt et al*., 2010], or fish teeth [*Martin and Scher*, 2004] have been proposed to reflect, with various degrees of success, the isotopic composition of Nd in the deep waters that bathe them. In principle this water column ε_{Nd} value is only affected by mixing of deep waters and could be used as an effective *x* axis for paleo tracer versus tracer plots. Northern source water has an unradiogenic value and is set in the surface North Atlantic like T and S. But the other ε_{Nd} "end-member" is set by sedimentary exchange in the Pacific with a radiogenic signal. This boundary condition in the deep Pacific is very different than the Southern Ocean surface fluxes of heat and salt, which define the southern deep water end-member. Unlike ε_{Nd}, other water mass tracers like $\Delta^{14}C$, CFCs, and $[O_2]$ depend on surface properties near the boundary conditions of T and S and can aid in constraining mixing ratios. A bottom up tracer has been a goal of the oceanography community since at least the days of GEOSECS where much time and effort were spent to characterize the inputs of Ra to the ocean in the deep Pacific. If ε_{Nd} could provide this view of the deep circulation, it would contain orthogonal information to T and S and be very useful in diagnosing water mass interaction. However, recent work has shown that as deep waters flow along margins they evolve in their ε_{Nd} value due to boundary exchange fluxes over and above their "end-member" inputs [*Lacan and Jeandel*, 2005; *Lacan et al*., 2012]. These processes add a nonconservative element to the water column ε_{Nd} values. Overall the use of ε_{Nd} as a tracer of water mass mixing is still under development. It has the distinct advantage of there being little chance of a biologically induced "vital effect," but the basics of the tracer in the modern water column are still to be uncovered [*Arsouze et al*., 2007; *Arsouze et al*., 2010]. Important work on where in the water column the ε_{Nd} value of foraminifera is set [*Elmore et al*., 2011] should be emphasized in the near term development of this tracer.

[21] Ideally the deep water mixing ratio tracer would come from a measure of salinity, temperature, or a proxy of either one. Indeed, one of the oldest problems in paleoceanography is how to separate the dual effects of temperature and $\delta^{18}O_{water}$ (salinity) from the single measurement of biogenic $\delta^{18}O$. For separate reasons, Emiliani [*Emiliani*, 1966] and Dansgaard [*Dansgaard and Tauber*, 1969] each assumed that the bulk of the glacial to interglacial signal in planktonic foraminifera is due to temperature. In contrast, Shackleton compared benthics and planktonics from the same core to show that $\delta^{18}O_{water}$ changes are actually about two third of the whole LGM signal [*Shackleton*, 1967]. Labeyrie used high latitude cores, where the freezing point is a defined temperature extreme, to make a similar point [*Labeyrie et al*., 1987]. Comparisons with the sea level record derived from surface corals have also been a useful way to normalize for the global portion of the $\delta^{18}O_{water}$ changes in benthic $\delta^{18}O$ data. Chappell and Shackleton [*Chappell and Shackleton*, 1986] demonstrated that the deep Pacific cooled by 2°C at the MIS 5e to 5d transition and then warmed again by the same amount only at the last termination. Adopting a similar strategy, and a better constrained coral-based sea level curve, Cutler et al. confirmed the Chappell and Shackleton result and found the deep Equatorial Atlantic warmed by ~4°C

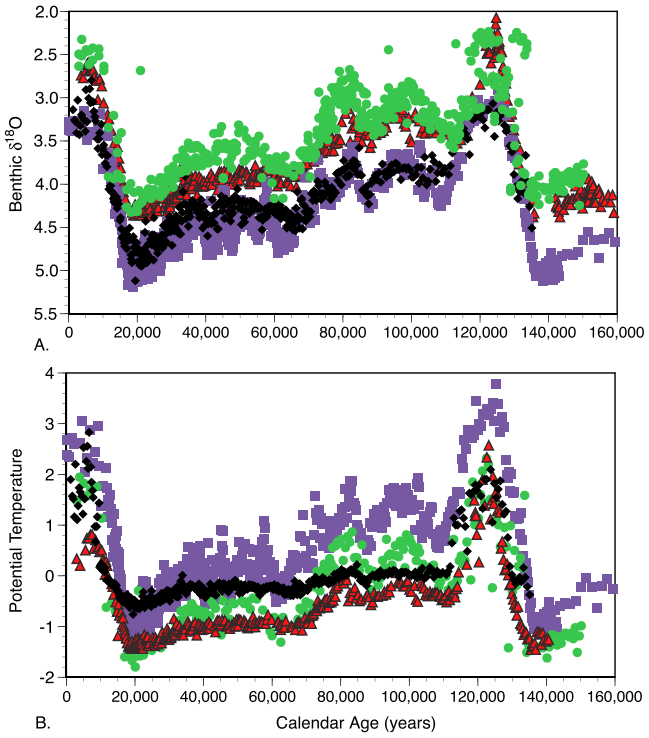

Figure 6. Deep ocean temperature changes from four high-resolution benthic $\delta^{18}O$ records (black diamonds, TR163-22, 2830 m [*Lea et al*., 2002]; red triangles with black outline, ODP1089, 4621 m [*Hodell et al*., 2003]; blue squares, MD95-2042, 3146 m [*Shackleton et al*., 2000]; green circles, EW9209-1JPC, 4056 m [*Curry and Oppo*, 1997]). Temperatures were estimated following the procedure of Chappell and Shackleton [*Chappell and Shackleton*, 1986] and Cutler et al. [*Cutler et al*., 2003]. I scaled the slope of the $\delta^{18}O_w$/sea level relationship for each core based on the local estimate of $\delta^{18}O_w$ at the LGM using pore fluids results [*Adkins et al*., 2002a] and a total sea level change of 120 m (TR163-22 $\delta^{18}O_w = 1.1‰$; ODP1089 $\delta^{18}O_w = 1.2‰$; MD95-2042 $\delta^{18}O_w = 0.9‰$, EW9209-1JPC $\delta^{18}O_w = 0.9‰$). This procedure eliminates the interlab offset in $\delta^{18}O$ measurements that can be seen in the MD95-2042 data by scaling the measured glacial to interglacial amplitude of d18O rather than the absolute values. There is a clear difference in the history of deep temperature between the Pacific (TR163-22) and the Atlantic (MD95-2042 and EW9209-1JPC) basins. Large Atlantic temperature changes at the MIS 5/4 boundary, and dropping into the LGM, are not found in the Pacific. The Southern Ocean (ODP1089, Atlantic Sector) is always the coldest water, though the deep North Atlantic cools to near freezing temperatures at the LGM, too.

at the last termination [*Cutler et al*., 2003]. The difference between a 2°C cooling at the 5e/5d shift and this 4°C Termination 1 warming is made up by about 2°C of cooling over the glacial period that was largely paced by Milankovitch cycles. These types of records, and some others from high-resolution benthic $\delta^{18}O$ data, are shown in Figure 6. An assumption in this work is that the scaling of $\delta^{18}O_{water}$ with sea level at the LGM [*Schrag et al*., 2002] holds for the whole glacial cycle. Waelbroeck extended this approach by constructing a global $\delta^{18}O_{water}$ curve for the last four glacial cycles using relative sea level changes measured during just the last glacial cycle and applying separate $\delta^{18}O_{benthic}$-sea level trends for glaciations and deglaciations [*Waelbroeck et al*., 2002]. These approaches have led to some very robust results (see Figure 6 and the discussion below), but they require that the global $\delta^{18}O_{water}$ signal be well mixed in the ocean during the slide into glacial maxima, an assumption that probably does not hold during deglaciation [*Gebbie*, 2012; *Skinner and Shackleton*, 2005]. Shackleton deconvolved the $\delta^{18}O_w$ signal from benthic forams by using the record of $\delta^{18}O$ in atmospheric O_2 and a tuning strategy to line up the sediment and ice cores [*Shackleton*, 2000]. His assumption of a constant Dole effect over the last glacial cycle makes his analysis less robust than others described here, but a principal conclusion that temperature comprises a significant fraction of the benthic foraminifera $\delta^{18}O$ variability has held up to subsequent scrutiny.

[22] Independent estimates of both the LGM deep ocean's $\delta^{18}O_{water}$ value and its salinity can be derived from pore fluid measurements of $\delta^{18}O$ and [Cl] in suitable cores. This idea of McDuff's [*McDuff*, 1985] was first successfully employed by Schrag and DePaolo [*Schrag and DePaolo*, 1993] and Schrag et al. [*Schrag et al*., 1996] in the deep Atlantic. Treating the sediment column like a sand packed pipe where tracer can diffuse and advect in only the vertical direction allows the measured profile in $\delta^{18}O$ and [Cl] at any site to constrain a model of the LGM bottom water values of temperature and salinity. The [Cl] to salinity conversion is straightforward and the $\delta^{18}O_{water}$ to temperature conversion only requires some benthic $\delta^{18}O_{CaCO3}$ measurements in the same core. Using a limited, but globally distributed set of cores, Adkins et al. [*Adkins et al*., 2002a] were able to constrain the T/S plot

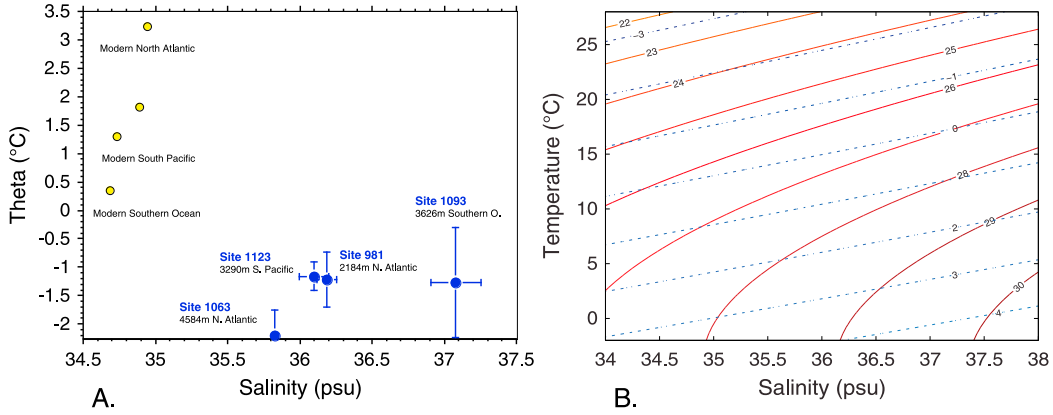

Figure 7. The relationship between temperature and salinity in the deep ocean and how these two work in the equation of state of seawater. (a) T/S plot based on the pore fluid measurements of [Cl] and $\delta^{18}O_w$ [*Adkins et al.*, 2002a]. Deep stratification in the modern ocean is largely controlled by temperature, but at the LGM salinity is the chief cause of density differences at these core sites. In addition, the modern meridional gradient of salt in the Atlantic reversed at the LGM to a dominant salty source from the Southern Ocean. (b) A calculated T/S plot with lines of constant sigma-theta (solid) and constant $\delta^{18}O_{CaCO3}$ (dashed). Lines of constant density curve with changing temperature because of the temperature dependence of the thermal expansion coefficient of seawater (known as "cabbeling"). At warm temperatures, isolines of $\delta^{18}O$ and σ_θ are parallel and benthic oxygen isotopes are a good proxy for density. At cold temperatures, the isolines cross. However, as the plot demonstrates, $\delta^{18}O_{CaCO3}$ is a linear combination of T and S (using the "Mixed Deep Water" line of Legrand and Schmidt [*LeGrande and Schmidt*, 2006] Table 1 to convert salinity into $\delta^{18}O_{water}$) and can be used as a conservative tracer of water mass properties.

for the LGM ocean using this technique (Figure 7a). This work confirmed the Schrag et al. inference that much of the deep ocean cooled to the freezing point at the LGM and found the surprising result that salty deep waters were produced in the Southern Ocean, not the North Atlantic, during this same time. The deep Atlantic salt gradient seen in Figures 3 and 4 evidently reversed sometime during the last glacial period. Exploring the implications of this result is part of the motivation for the last section of this paper.

[23] Other tracers for deep ocean temperature have also been investigated. The Mg/Ca ratio in planktonic foraminifera has seen widespread use in recent years as a robust (if postdepositional dissolution effects can be minimized or calculated) tracer of SST [*Elderfield and Ganssen*, 2000; *Rosenthal et al.*, 2000]. However, only a few studies have tried to use this technique in benthic forams. Martin et al. measured the last glacial cycle in the deep Pacific and found temperature changes that are broadly consistent with Chappell's and Cutler's results [*Martin et al.*, 1998]. During MIS 3 and 4 these authors found deep ocean temperature shifts that correlate with pCO_2 changes measured in Antarctic ice cores. An elegant comparison of the CO_2-temperature sensitivity during Termination 1 and the glacial period demonstrates that nearly all of the glacial age pCO_2 changes can be attributed to the temperature dependence of CO_2 solubility in the ocean [*Martin et al.*, 2005]. Terminations, on the other hand, have too steep a temperature sensitivity to be explained by thermodynamics alone and must have CO_2 exchanges between reservoirs as part of their explanation. Skinner et al. have used the Mg/Ca ratio measured in the benthic species *Globobulimina affinis* to constrain time series of deep ocean temperature off the Iberian margin [*Skinner and Elderfield*, 2007]. They find large (~1.5°C) shifts associated with Heinrich Events where the water at ~2600 m both warms and cools by about 1°C. Recently, Elderfield et al. have shown, from a long record of coupled benthic $\delta^{18}O$ and Mg/Ca from the South Pacific, that each glacial maximum reached very close to the freezing point for the last 1.4 Ma [*Elderfield et al.*, 2012].

[24] There are several promising new tracers of ocean temperature that could play an important role in future reconstructions of deep ocean circulation. Mg/Li ratios in foraminifera [*Bryan and Marchitto*, 2008] and deep-sea corals [*Case et al.*, 2010] are correlated with bottom water temperature. As both Mg and Li show large increases in the centers of calcification of biogenic carbonate, taking their ratio helps to normalize out this nontemperature-dependent aspect of Mg incorporation into skeletons. The tracer has not been used to monitor past ocean conditions yet, but it clearly holds some promise. Noble gas measurements in terrestrial aquifers have been usefully employed to constrain the LGM tropical temperature change [*Stute et al.*, 1995]. In a new twist on this idea, Kr/N_2 gas concentration ratios in ice cores are proposed to constrain the mean deep ocean temperature at any one time [*Headly and Severinghaus*, 2007; *Ritz et al.*, 2011]. Assuming that these two gases are conserved, the gravitational fractionation effects can be accounted for, and employing a mass balance model, LGM values from GISP2 show a mean ocean temperature change of 2.7 ± 0.6°C. Unlike the aquifers, the inherent stratigraphy of ice cores should allow for this approach to provide time series of average deep ocean change in the future. Finally, a new approach to the stable isotopes of oxygen and carbon in biogenic skeletons has been pioneered by John Eiler and his group at Caltech. The relative propensity for ^{13}C and ^{18}O atoms to form bonds with each other in $CaCO_3$, over and above a stochastic distribution based only on their relative abundances, has a temperature-dependent equilibrium constant [*Ghosh et al.*, 2006]. Carbonates from inorganic precipitation in the lab and a wide variety of

biogenic skeletons show the same sensitivity to temperature change for this clumped isotope, or Δ_{47}, ratio. Due to the analytical precision required to get 1–2°C error bars, the technique is sample intensive and will probably not be a good high-resolution paleo-temperature tool in the near future. However, the thermometer is independent of the $\delta^{18}O_{water}$ value and does show great promise in systems where large samples can be collected [*Eiler*, 2011; *Thiagarajan et al*., 2011]. This new technique is sure to advance our understanding of past deep ocean behavior via judicious application to problems where a few data points will make a lasting impact.

3.3. Circulation Rate and Volume Transport Tracers

[25] To understand the role of the deep ocean in past climate change, we need more than the volumes and distributions of past water masses; we need constraints on the rates of deep water mass circulation. From the earliest days of the field, models [*Sarmiento and Toggweiler*, 1984] and theories [*Broecker et al*., 1990b] have called on changes in the rate of overturning of the deep ocean to play an important role in glacial to interglacial, and rapid, climate changes. This approach has been expanded to include calculations of changing residence times of ocean tracers, either through reduced overturning or through increased ocean reservoir size [*Skinner*, 2009]. Several tracers with inherent rate information inform our understanding of the modern circulation rate in the deep sea. Chlorofluorocarbons and bomb ^{14}C rely on time varying boundary conditions at the air-sea interface to label newly forming deep and intermediate waters. Natural ^{14}C and ^{39}Ar rely on the radioactivity of the tracers themselves to map the distribution of deep and intermediate water ventilation ages. ^{3}H (and now excess ^{3}He) uses both the radioactive decay of the tracer and its time varying input history at the surface ocean to estimate the ventilation time scale of the ocean interior. For the most part, paleoceanography relies only on the radioactive tracers ^{14}C and $^{231}Pa/^{230}Th$ to retrieve age estimates from this class of age tracer. I discuss other physically based, rather than radioactivity based, age and rate tracers in detail later.

[26] Radiocarbon ventilation age estimates in the past ocean are problematic because ^{14}C is one of our most useful chronometers. A single age measurement cannot both constrain the time since the carbonate sample formed and the ^{14}C age of the water in which it grew. For surface waters between 40°N and 40°S, it is often a good assumption that the water ^{14}C age (the so-called "reservoir age") has not changed much from the modern value of ~400 years [*Bard*, 1988], with the notable exceptions of the Younger Dryas and Heinrich Event 1 in the North Atlantic [*Siani et al*., 2001; *Waelbroeck et al*., 2001]. But for the deep ocean, where water ^{14}C ages can exceed 2000 years, this is not a good assumption. With the advent of Accelerator Mass Spectrometry in the late 1980s, this problem began to be solved. This new technique decreased the detection limit for $^{14}C/^{12}C$ ratios such that measuring the age difference between contemporaneous planktonic and benthic foraminifera became possible on a reasonable number of picked shells [*Broecker et al*., 1988; *Duplessy et al*., 1989; *Shackleton et al*., 1988]. The key insight is that all forams from the same depth in a core can be assumed to be of the same calendar age, so that ^{14}C differences between planktonics and benthics remain constant even as they all decay with time. Early results were very noisy but they all generally showed a glacial Pacific that was equal to or slightly older than today, and a glacial Atlantic that was clearly older than the modern ocean [*Adkins and Boyle*, 1997; *Broecker et al*., 1990a]. There has been a renaissance in this method over the last several years [*Ahagon et al*., 2003; *Broecker et al*., 2006; *Broecker et al*., 2004; *Burke and Robinson*, 2012; *De Pol-Holz et al*., 2011; *Galbraith et al*., 2007; *Ingram and Kennett*, 1995; *Keigwin and Schlegel*, 2002; *Lund et al*., 2011b; *Marchitto et al*., 2007; *Sikes et al*., 2000; *Skinner et al*., 2010; *Sortor and Lund*, 2012; *Stott et al*., 2009; *Stott*, 2007; *Thornalley et al*., 2011] as the importance of picking benthic abundance maxima to minimize scatter from bioturbation [*Keigwin and Schlegel*, 2002] and comparing multiple species of planktonic forams from the same core depth interval [*Broecker et al*., 1999] has been recognized. Some areas, like the Eastern Equatorial Pacific [*Broecker et al*., 2004], still return conflicting data but the measurement of the abyssal (>4000 m) North Atlantic as much older than today seems robust [*Keigwin*, 2004]. A picture is emerging for the LGM Pacific where there are relatively well-ventilated intermediate waters underlain by deep and abyssal waters that increase in age with depth to > ~2000 years at the LGM [*Galbraith et al*., 2007; *Sikes et al*., 2000].

[27] However, these results are not without controversy. Broecker has found individual cores from the deep Pacific that have the same B-P age during ice age intervals as the modern ocean at that site [*Broecker et al*., 2004]. In intermediate waters, the debate has been especially problematic. Marchitto et al. [*Marchitto et al*., 1998] document very large swings in the $\Delta^{14}C$ of water at ~700 m off the coast of Baja California. This foraminifera record is exceptional because it is one of the first to bypass the use of benthic minus planktonic ages and instead use the independent age model of the core to calculate $\Delta^{14}C$ from benthic ^{14}C ages alone. The continuous record this approach provides is impressive as the $\Delta^{14}C$ swings match the atmospheric record of both $\Delta^{14}C$ and pCO_2. However the implied ~450‰ difference between the atmosphere and the water at 700 m is difficult to reconcile with whole ocean mass balance arguments. Short of cutting off air-sea gas exchange at these latitudes entirely, even a completely radiocarbon dead deep ocean (−1000‰) cannot sustain the size and the duration of the Marchitto signal [*Hain et al*., 2011]. Further confounding this problem is that a similar signal has been observed in the Indian Ocean [*Bryan et al*., 2010]. However, several sites that should also have the intermediate-mode water signal if it is present off Baja do not see the same dramatic changes, either off of Chile [*De Pol-Holz et al*., 2011] or in the North Pacific [*Galbraith et al*., 2007; *Lund et al*., 2011b]. One controversial solution to these different signals is that ^{14}C dead CO_2 clathrates destabilize at specific locations around the globe during times of deep ocean warming, thus contributing a very depleted $\Delta^{14}C$ signature to many bottom waters [*Stott and Timmerman*, 2011]. Fortunately a second archive, besides forams, has also been able to measure the past $\Delta^{14}C$ content of intermediate and deep waters since the LGM.

[28] Surface corals have been useful archives of past $\Delta^{14}C$ information since Bard's and Edwards' pioneering work in the early 90s [*Bard et al*., 1990; *Edwards et al*., 1993]. Rather than using ^{14}C age differences, the combination of U-series and ^{14}C dating frees radiocarbon from being a chronometer and allows it to be a tracer of the $\Delta^{14}C$ of DIC. For

deep-sea corals, this combination of radioactive clocks gives us information much like the *y* axis in Figure 4c [*Adkins et al*., 2002b]. When applied to fossil corals that grew sometime during the past ~40,000 years, we can potentially constrain the rate of past deep ocean circulation [*Adkins et al*., 1998; *Mangini et al*., 1998]. While the analytical precision of past $\Delta^{14}C$ is markedly increased with deep-sea corals over their benthic-planktonic counterparts, the data are still hampered by both a lack of understanding of deep water end-member $\Delta^{14}C$ changes through time and a lack of LGM-aged corals from deep and abyssal depths—though a few points from the Southern Ocean exist for the deglaciation [*Goldstein et al*., 2001; *Robinson and van de Flierdt*, 2009]. Deep-sea corals and sediments are complimentary archives, as corals can constrain rapid changes in the deep ocean more accurately, but benthic/planktonic difference data leads more naturally to longer time series and the greater context these records bring to the problem. With these caveats in mind, several interesting patterns have emerged. A time-depth section of $\Delta^{14}C$ variability at ~40°N in the western basin of the Atlantic shows very large swings associated with rapid climate changes [*Robinson et al*., 2005]. The LGM deep Atlantic, constrained mostly by benthic forams [*Keigwin*, 2004], was over 150‰ more depleted in $\Delta^{14}C$ relative to its contemporaneous atmosphere than it is today. H1 is a time of rapid fluctuations in "old" and "young" signatures above ~2000 m, but with much less variability below this depth, though the deep data density is not great. The Younger Dryas is a time of whole water column $\Delta^{14}C$ depletion that is followed by a fairly rapid return to better ventilated $\Delta^{14}C$ values at the end of the event [*Eltgroth et al*., 2006]. In the South Atlantic, the Younger Dryas, H1, and H2 are times where deep-sea corals show nearly stagnant ventilation over thousands of years at about 1000 m water column depth [*Mangini et al*., 2010]. This dramatic result also implies that the YD stagnation lasted well into the Mid-Holocene. For the same reason that Hain et al. [*Hain et al*., 2011] criticized the Marchitto result from lower thermocline waters in the Equatorial Pacific, it is hard to imagine how these large $\Delta^{14}C$ depletions off Brazil, and the stagnant water circulation they imply, can be sustained by the ocean-atm $\Delta^{14}C$ system. It is possible that some component of this deep-sea coral result may come from the fact that the sample patches grew near ^{14}C-dead methane seeps. Independent checks are necessary to fully understand what the implications of these data.

[29] A recent study from deep-sea corals in the Drake Passage has gone a long way to resolving some of the confusion in the deglacial radiocarbon record. Conflicting reports of deep and intermediate water mass ages have been discussed above. With a new record from Upper Circumpolar Deep Water (UCDW) and a summary of previous records from in and around the Southern Ocean, Burke et al. show a radiocarbon stratified ocean at the LGM and in the early deglaciation [*Burke and Robinson*, 2012]. Late in Heinrich Stadial 1, the stratification was dramatically removed as most of the deep records "mix" to very similar $\Delta^{14}C$ values. Intermediate waters remained younger than deeper waters across this event, thus still contradicting the Baja margin data set and interpretation. This is the same time that Robinson et al. report an invasion of older ^{14}C waters above 2000 m in the North Atlantic [*Robinson et al*., 2005]. The available radiocarbon data imply that during the Heinrich Stadial the deep ocean became well mixed and southern sourced intermediate waters spread northward in the Atlantic.

[30] Radiocarbon is not the only chemical tracer with rate information based on its radioactive decay in the water column. Down core measurements of the $^{231}Pa/^{230}Th$ ratio in the North Atlantic show changes in the overlying water's value that are related to the strength of the overturning circulation [*McManus et al*., 2004]. The principles behind the technique were established while searching for an absolute chronometer beyond the ^{14}C age window and were first applied by Yu et al. [*Yu et al*., 1996] in a basin wide study of LGM Atlantic sediments. ^{231}Pa and ^{230}Th are produced from separate uranium parents in the water column, but their different chemical reactivity with particles in seawater allows ^{231}Pa to be preferentially transported by the flow field away from its production region, as compared to the more reactive ^{230}Th. Therefore, an Atlantic Ocean that is actively transporting ^{231}Pa out of the basin via the overturning circulation will have $^{231}Pa/^{230}Th$ ratios in the sediments that are below the production ratio. A more sluggish circulation will have ratios closer to that set by their soluble uranium parents. Yu found that the LGM Atlantic exported ^{231}Pa from the basin about as efficiently as the modern does. McManus largely confirmed this result but also showed that Heinrich Stadial 1 was a period of near stagnant overturning at the Bermuda Rise. At this site, the Younger Dryas episode was less vigorous in its overturning than the modern, or even the LGM, but it was not nearly the collapse seen at H1.

[31] This H1 result has been challenged [*Keigwin and Boyle*, 2008] on the basis that ^{231}Pa is preferentially scavenged by silica from diatom frustules, regardless of the deep ocean overturning rate [*Walter et al*., 1997]. If Heinrich events are times of larger or more frequent diatom blooms, then the $^{231}Pa/^{230}Th$ rate tracer could be compromised. A more comprehensive follow-up study to the original McManus paper measures a depth transect of cores in the North Atlantic from both the Eastern and Western basins and finds largely coherent signals between them [*Gherardi et al*., 2005]. A major result from this work is that transport at intermediate depths, corresponding to GNAIW as defined by nutrient tracers, was stronger than it is today. As the $^{231}Pa/^{230}Th$ tracer is more easily reset to its scavenging-determined value at intermediate depths [*Gherardi et al*., 2009], the measured deficit of ^{231}Pa relative to ^{230}Th in this work seems to be a robust indicator of vigorous transport of GNAIW at the LGM. The H1 time slices from Gherardi et al. confirm the earlier results, but they still allow for export of North Atlantic waters to the south during this deglacial event. Both forward [*Marchal et al*., 2000] and inverse models [*Burke et al*., 2011] have shown that the utility of this volume transport rate tracer will be substantially enhanced with a better understanding of the scavenging rate constants for both radionuclides. This later point is emphasized in work from the Southern Indian Ocean where sedimentary $^{231}Pa/^{230}Th$ ratios are interpreted as monitoring the water mass closest to the bottom, rather than as an integral of the whole water column [*Thomas et al*., 2006]. The assumed balance between advection and particulate-dissolved partitioning of ^{231}Pa is a crucial piece of the interpretation of this radionuclide data.

[32] Radioactive clocks are not the only way to extract circulation rate information from the sedimentary record. Because its value is a linear combination of temperature and

salinity effects, the $\delta^{18}O$ of benthic forams can be a direct tracer of seawater density. At shallower depths where warmer deep waters are not strongly affected by the temperature dependence of the thermal expansion coefficient, lines of constant density and lines of constant carbonate $\delta^{18}O$ are roughly parallel on a seawater T/S plot, though this is not true at the colder abyssal water depths [*Lynch-Stieglitz et al*., 1999b] (Figure 7). When combined with the geostrophic equation, slopes of isopycnals across a bathymetric gap or an ocean basin are a measure of water mass transport. Using the $\delta^{18}O$ of benthics to measure the past slopes of isopycnals in the Florida Straits, the LGM had a one third reduction in transport through this key region of the Gulf Stream flow [*Lynch-Stieglitz et al*., 1999a]. One interpretation of this data is that the wind-driven portion of the total flow through the Straights has been constant and the one third reduction is due to a near elimination of the overturning circulation component. In other words, the LGM NADW flux, now in actual Sverdrups of flow not as a relative change in a passive tracer value, was almost completely eliminated. Recent work supports a similar lowering of flow in this region during the Younger Dryas event [*Lynch-Stieglitz et al*., 2011], though for all these results it is important to recognize that some portion of the northward flow is east of the Bahamas and not through the Florida Straits and that this technique only measures the baroclinic portion of the northward transport. A disagreement in the tracers has developed for the LGM across basin density estimates for the South Atlantic [*Lynch-Stieglitz et al*., 2006]. Lynch-Stieglitz et al. find that the tilt of isopycnals above 2000 m at 30°S reversed from southward flow today to northward or no-flow at the LGM. For this result to be reconciled with the Gherardi $^{231}Pa/^{230}Th$ North Atlantic profile discussed above, there must be water mass convergence somewhere in the LGM tropical Atlantic, a situation that is not easy to reconcile with the LGM $\delta^{13}C$ evidence [*Sigman et al*., 2003]. Clearly, more work needs to be done to resolve these issues.

[33] Direct measurements of current flow are an important tool in modern physical oceanography. In paleoclimate, a local measure of the speed of currents coupled with other tracers of water mass origin can enhance our understanding of deep circulation rates, though local velocities do not scale to the larger tracer transport very well. Looking at just the terrigenous fraction of the sediments and measuring the mean size of the sortable silt (SS, 10–63 μm) can give a good estimate of relative bottom current speed [*McCave et al*., 1995]. Sediments larger than this fraction tend not to move in the range of bottom current sheer stresses and smaller sediments tend to aggregate and not behave according to simple physical laws [*McCave and Hall*, 2006]. The SS parameter shows an abrupt slowing of deep currents at the end of MIS 5e in the deep North Atlantic, with this pattern of slow speeds during cold intervals continuing through the whole glacial cycle off of the Iberian Margin [*Hall and McCave*, 2000]. Deglacial records from the North Atlantic show slower bottom waters between 2800 m and 4000 m water depth during the H1 and YD events and faster waters during the Bolling-Alerod [*Manighetti and McCave*, 1995]. These data agree nicely with the Pa/Th record from McManus et al. discussed above. In the future, the most promising use of sortable silt estimated current speeds may be to find the depths of the deep western boundary currents during climate transitions [*Evans et al*., 2007]. While local currents are not a good estimate of total transport, they can give us a coherent picture of the shoaling and deepening of boundary currents that could be usefully linked to changes in surface forcing.

4. Discussion

4.1. Extracting Quantitative Circulation Information From Past Tracers

[34] In the early days of paleo deep water hydrography, it was important to make tracer data a proxy for another species that has more relevance for the climate system. Cd/Ca and $\delta^{13}C$ were seen as proxies for $[PO_4]$. Ba/Ca was interpreted as alkalinity. However, the advent of computer models of varying complexity makes it possible to think about paleo tracers not as substitutes for anything, but instead as unique tracers in their own right. Given the correct set of boundary conditions, and an accurate description of the nonconservative behavior of a tracer, GCMs provide a way to extract quantitative information about past circulation from the tracer fields themselves. One success in this area was the comparison of four models run with LGM boundary conditions as part of the PMIP program (paleo model intercomparison project). Otto-Bliesner et al. found that all four models had similar surface climates when run to steady state, but that two models had a more vigorous overturning circulation in the Atlantic while two had a weaker one [*Otto-Bliesner et al*., 2007]. The $\delta^{13}C$ distribution and the T/S plot for these two different types of deep ocean behavior correspond to different sea ice dynamics in the model pairs. The two "correct" models have a shoaled version of GNAIW and salty waters produced in the Southern Ocean. Each of these features is driven by sea ice dynamics at the surface. In this work, the deep tracers are able to distinguish important differences in the climate physics that still led to similar looking steady-state atmospheres, but very different looking deep oceans.

[35] As quantitative statements of all that one knows about both the data and the model's ability to simulate the actual circulation, inverse models are perhaps the most important route forward for paleoceanography of the deep circulation. In the modern ocean, the advent of large data sets and sophisticated models coupled to powerful computers allows for the inversion of T and S data for deep circulation patterns and fluxes [*Ganachaud and Wunsch*, 2000; *Schlitzer*, 2002]. This description of basic circulation physics, mostly geostrophy, in an inverse framework is the gold standard for extracting quantitative information from tracer distribution, partly because it allows one to quantitatively state the errors in both the data and the model. However, the efforts that currently exist in the literature have largely demonstrated that the LGM data set for the deep ocean is too sparse to say much about the past circulation in this inverse context [*Huybers et al*., 2007; *LeGrand and Wunsch*, 1995; *Marchal and Curry*, 2008]. However, Marchal and Curry demonstrate one exception to this conclusion for the $\delta^{13}C$ distribution at the LGM. If they assume that only advection and organic matter remineralization act to determine the abyssal $\delta^{13}C$ (i.e., no vertical diffusion), then the LGM and the modern circulations had to be different. In some cases, models have been used to probe the sensitivity of tracers to other processes, like scavenging rate constants for Pa/Th [*Burke et al*., 2011; *Marchal et al*., 2000] and boundary exchange for ε_{Nd} [*Arsouze et al*., 2007].

These tracer-specific efforts are useful and can guide future work or even produce "calibrations" for the transformation of tracer changes into circulation changes. However, the overwhelming conclusion from the paleo inverse models run to date is that the past tracer distribution cannot discount the null hypothesis that the past deep circulation was not different from that of the modern ocean.

[36] Is this the final answer on extracting quantitative information from paleo deep ocean tracers? There certainly seems to be a different distribution of tracer in the LGM ocean (Figure 5) and wide fluctuations in tracers from time series spanning the last glacial and Termination 1. However, placing circulation arrows on this picture ignores other processes besides tracer advection and can be especially problematic with tracer patterns that have no inherent time information. Perhaps there is a way forward that does not ask too much of a sparse data distribution, but that also does not ignore much of what has been learned in the last decades about the turbulent nature of deep ocean circulation. We have seen how along isopycnal tracer analysis can yield simple, but powerful, statements about the circulation rate. However, most paleo data are more easily structured in depth coordinates than in density space. In the 1960s, Walter Munk presented a solution to these problems in a 1-D balance of vertical diffusion and advection he called "Abyssal Recipes" [*Munk*, 1966]. This influential work demonstrated how the combination of a single conservative tracer and $\Delta^{14}C$ measurements in a Pacific Ocean depth profile could separately constrain the local vertical upwelling rate and the local vertical diffusivity of tracer in the ocean interior. A profile of a conservative tracer constrains the ratio of upwelling to vertical diffusion at that site. The $\Delta^{14}C$ profile adds a second constraint with no new unknowns to this problem and allows for the separation of the upwelling/diffusion ratio into its component parts. The key is an assumption that the ocean behaves as a one-dimensional fluid, something we clearly know is not the case today. However, Munk's numbers of 1×10^{-4} m^2/s and ~4 m/yr, for vertical diffusivity and a global upwelling rate respectively, have stood the test of time, possibly because these are the implied diffusivity and upwelling for 20 Sv of new deep water formation and a return flow that is evenly spread over the whole ocean area.

[37] The review sections above demonstrate that measurements of T, S, and $\Delta^{14}C$ are now possible for the past ocean as well, thus potentially providing all the information a Munk-like analysis would need. In fact, the $\delta^{18}O$ of benthic forams themselves are a conservative tracer, even without separation into temperature and $\delta^{18}O_w$/salinity/ice volume components. As a linear combination of two conservative tracers, $\delta^{18}O$ values in biogenic carbonate are set at the surface and mix conservatively in the ocean interior. This is true even for the coldest regions of the deep ocean where the $\delta^{18}O_{calcite}$-density relation breaks down (Figure 7). Even if $\delta^{18}O_{benthic}$ is not a proxy for density at cold temperatures, it is always transported and diffused like all other conservative tracers; it is itself an excellent marker of water masses. Keigwin et al. used a version of this idea and the Abyssal Recipes approach to constrain the ratio of diffusion to upwelling in the Pliocene ocean [*Keigwin et al*., 1979]. In a recent paper, we have used $\delta^{18}O_{benthic}$ as a conservative tracer with a modified version of its water mass budget to constrain the deep circulation characteristics of the LGM Southern Source waters [*Lund et al*., 2011a].

[38] Recognizing that the $\delta^{13}C$ data in Figure 5 also have $\delta^{18}O$ data associated with them, we pointed out that profiles of benthic $\delta^{18}O$ in the LGM Atlantic [*Curry and Oppo*, 2005; *Keigwin*, 2004] and Indian [*Kallel et al*., 1988] have a distinct kink at ~2000 m water depth (Figure 8b). For a conservative tracer, this sharp vertical gradient represents a water mass boundary. We constructed a whole water mass conservative tracer mass balance, rather than just a 1-D balance as in "Abyssal Recipes," using this demarcation for the upper lid of northward flowing southern source water (Figure 8a). The amount of $\delta^{18}O_{benthic}$ in the water mass north of 30°S can only change via transport of tracer into the volume (equivalent to the physical oceanographer's overturning stream function) and the diffusion of tracer across the southern source-northern source water mass boundary defined by the vertical $\delta^{18}O_{benthic}$ kink. In the modern ocean, this kink sits in the core of AABW ($\gamma n = 28.15$) and is the depth below which flow is to the north. The difference from Munk's approach is that now we are constraining the ratio of tracer transport to tracer diffusion across the whole water mass, rather than assuming a local 1-D balance. Comparing the modern and LGM tracer balances in this way, we found that the ratio of transport to diffusion increased at the LGM by a factor of ~8, with a minimum change (given the errors involved) of a factor of 2. As it is hard to imagine the circulation of the deep-sea having the energy to spin eight times faster [*Ferrari and Wunsch*, 2009], we interpret this result as a dramatic drop in the vertical diffusivity of tracer between the northern and southern LGM deep water masses. This "middle way" between full GCMs and their attempt to reconstruct the velocity vector at every grid point, and the simple statements that changed tracer distributions mean changed fluxes, yields a large and robust result (at least until more water column profiles of $\delta^{18}O_{benthic}$ are collected).

[39] There are at least two ways that reduced vertical mixing between deep water masses in the Atlantic could have come about at the LGM. Today the profile of vertical diffusivity in the ocean interior is at a minimum at middepths and then increases towards the bottom. It is widely believed that the interaction of deep internal waves with the rough topography of ridges and seamounts leads to this enhanced mixing at depth [*Polzin et al*., 1997]. As this feature is almost certainly independent of the glacial-interglacial cycles, shoaling of the boundary between northern and southern source water masses at the LGM would naturally lead to lower vertical diffusivity by pushing the boundary into the low mixing portion of the ocean interior. Today NADW and AABW interact at depths where mixing is vigorous, but at the LGM this was not true (Figure 5). The observed water mass geometry at the LGM would naturally lead to less vertical mixing and a lower ratio of transport to diffusion [*Lund et al*., 2011a].

[40] In an LGM ocean that is salinity stratified, the equation of state of seawater itself provides a second way to achieve less mixing between these water masses. As pointed out in Figure 3, today NADW and AABW share isopycnals in the ocean interior due to the competing tendencies of heat and salt on the density of these water masses. At the ocean surface modern, NADW is denser than AABW, but referenced to 3000 m water depth the north-south density contrast is reversed. The saltiness of NADW that makes it denser at the surface is compensated for by the larger amount of work it takes to push warmer waters down to high pressure. At depth, the coldness of AABW causes it to be denser than does the

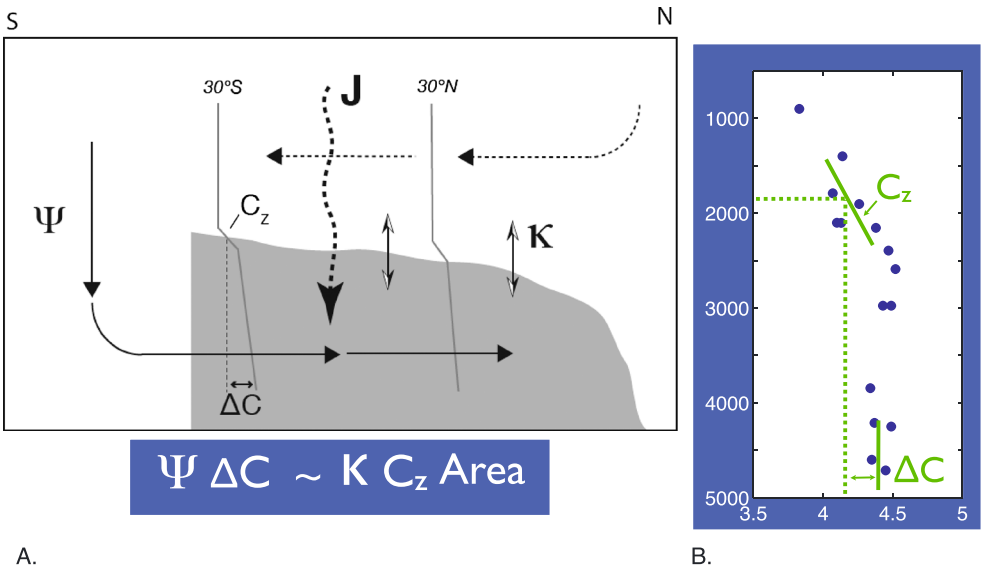

Figure 8. (a) Schematic of the LAF [*Lund et al.*, 2011a] $\delta^{18}O_{CaCO3}$ tracer conservation idea. In a latitude-depth section, the gray area represents southern source water with its upper boundary defined by a constant $\delta^{18}O_{benthic}$ value where the vertical gradient in $\delta^{18}O$ is a maximum, its southern boundary defined by the location of a $\delta^{18}O_{benthic}$ profile, and the bottom boundary at the sediment-water interface. The conservative tracer can only be changed in the control volume by transport (Ψ in units of m^3/s) at the southern boundary and by diffusion (K in units of m^2/s) across the upper contact with northern source water. The transport-diffusion flux balance at steady state is defined by Ψ multiplied by the tracer values going in (ΔC), balanced by K multiplied by the tracer concentration gradient at the upper boundary (C_z), multiplied by the area of the upper boundary (a). A profile of $\delta^{18}O_{benthic}$ at the LGM (B.) contains the values of both C_z and ΔC such that the profile defines the ratio of Ψ/K (see text and *Lund et al.* [2011a]).

saltiness of NADW. This means that there is a class of isopycnals that outcrop in both deep water formation regions and tracer diffusivity along isopycnals will work to mix the effects of separate surface boundary processes in the north and the south. The diffusion coefficient for this tracer flux is ~10^7–10^8 times higher than cross isopycnal mixing, such that today NADW and AABW can readily exchange tracer values between them even in regions of low vertical mixing. At the LGM where the deep ocean seems to be stratified by salt instead of heat (Figure 7a), this sharing of isopycnals between water masses would not happen. The mixing of tracer between the water masses would only come from cross isopycnal processes, or mechanically driven mixing in surface regions where both water masses outcrop near each other. The overall mixing of northern and southern water masses at the LGM would therefore be much lower than it is today. It is probable that both the mechanical and the thermodynamic explanations for lower vertical mixing at the LGM are partially responsible for the ~8× increase in the ratio of transport to diffusion. This insight into past mixing processes demonstrates the power of having truly conservative tracers of past ocean behavior.

4.2. Summary of the Glacial Deep Circulation

[41] Given the above review, there are a few robust and salient features of the LGM deep ocean that require some explanation. Our view is heavily biased towards the Atlantic because that is where most of the records can be collected (Figure 9). At the LGM, this basin seems to have been filled with a nutrient-rich water mass from the south at the expense of the $\delta^{13}C$-rich and Cd/Ca-poor water mass formed in the north. The boundary between these two shoaled from ~4000 m today to ~2000 m at the LGM. Associated with this switch, the radiocarbon content of the deep Atlantic dropped significantly and the mixing between these main water masses decreased. These changes were accompanied by a switch from warm-salty northern source waters and cold-fresh southern source waters, to a deep ocean filled with cold-salty water from around Antarctica.

[42] Much of the available benthic stable isotope data from across all ocean basins suggests that the deep ocean's two-cell structure shown in Figure 9 was much more pronounced and separated at the LGM than it is today (Figure 10). As compiled by Duplessy et al. [*Duplessy et al.*, 2002], there is a very different trend in $\delta^{18}O$ versus $\delta^{13}C$ at the LGM than is observed in the modern ocean. In this sort of tracer-tracer plot, three water masses that mix with each other are connected by data points between the end-members at the points of the triangle. Waters from the North Atlantic and Pacific Oceans fall along a tracer mixing line, while Southern Ocean cores are in a separate corner of the plot disconnected from the rest of the ocean. Of course the limited sampling of the LGM ocean by sediment cores might bias the interpretation of this figure, but there is little hint of southern source waters interacting with either the Atlantic or the Pacific waters. Benthic $\delta^{13}C$ goes to lower values as waters from the Atlantic mix with waters from the Pacific, presumably because of the remineralization of raining organic matter and water mass aging along this flow path. The Atlantic $\delta^{18}O$ is higher than the Pacific benthics, but pore water data show that the $\delta^{18}O_w$ in the Atlantic is lower than the Pacific. This means that the heavy $\delta^{18}O$ signal must be the result of colder temperatures in the Atlantic. Southern sourced $\delta^{18}O$ is also heavy (and cold), but its higher salinity

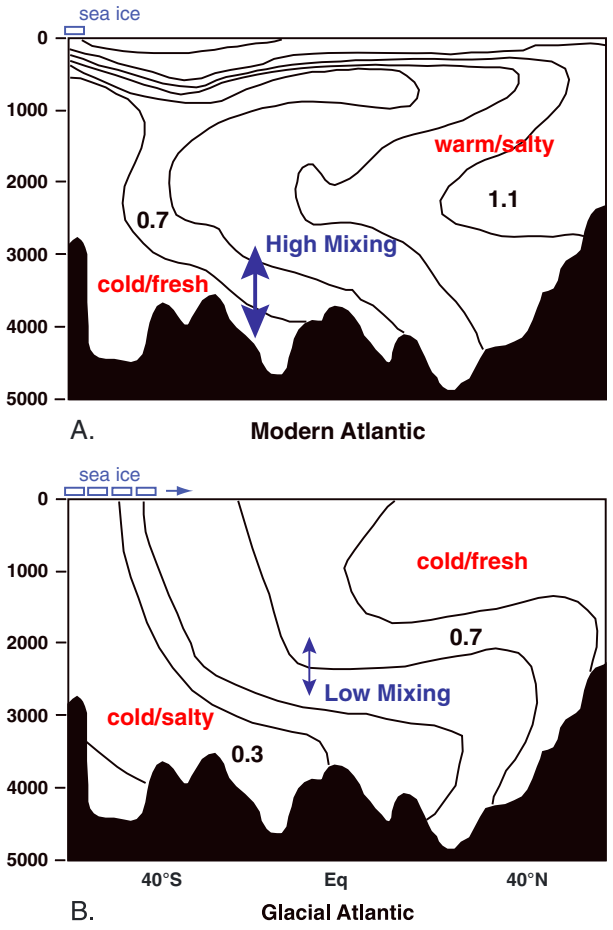

Figure 9. A summary of the important features of the LGM deep (b) ocean as contrasted with the modern Western Atlantic section (a). Isolines are for the $\delta^{13}C$ of DIC and are redrawn after Duplessy et al. [*Duplessy et al*., 1988]. Shoaled northern source water is fresher than the more dominant southern sourced water such that the LGM salt gradient at depth has reversed from the modern. Enhanced vertical mixing near the bottom of the ocean at the NADW/AABW boundary in the modern ocean is shown as a larger double-headed arrow. Increased sea ice export out of the Southern Ocean deep water formation region is one way to make these waters saltier. Reduced melting of the land-based ice around Antarctica is another (see text and *Miller et al*. [2012]).

keeps it denser than North Atlantic waters. One explanation for the $\delta^{18}O$-$\delta^{13}C$ pattern in Figure 10 is that the deep southern sourced cell does not mix with a shallower circulation that has both North Atlantic and North Pacific deep water sources and that there is some deep stratification between these water masses in the LGM ocean. Today's two-cell structure of the overturning circulation in the Atlantic seems even more pronounced and separate at the LGM.

[43] While the goal of this paper is to review the state of the deep ocean circulation during the last glacial, it is instructive to briefly consider the implications of the summary above for past atmospheric CO_2 levels. Toggweiler [*Toggweiler*, 1999] discussed how reduced mixing between north and south sourced deep waters in a seven-box model can lower atmospheric CO_2, and explained the deep chemical divide seen in benthic $\delta^{13}C$ [*Ninnemann and Charles*, 2002] in this manner. However, neither *Toggweiler*, 1999 nor the Harvardton Bears papers directly considered the crucial role of carbonate compensation in setting pCO_2 [*Broecker and Peng*, 1987]. Recent box modeling work shows that this process is also interrelated with the biological and physical "pumps" of CO_2 into the deep during the glacial [*Hain et al*., 2010]. Hain's modeling also emphasizes the coupled effects of circulation and productivity in the Southern Ocean and shows that Toggweiler's models were probably too sensitive to circulation changes alone. Probably the most useful single statistic for monitoring this coupled behavior is the total inventory of preformed nutrients in the glacial ocean [*Sigman et al*., 2010]. These nutrients, which leave the deep water formation regions without fueling organic matter production, represent a leak in the biological pump and their inventory is directly related to the amount of CO_2 left in the atmosphere (Figure 2c). Both the utilization efficiency of nutrients in the high latitudes and the circulation of the deep ocean affect the integral of preformed nutrients in the deep, sometimes in nonintuitive ways. For example, given a constant gas exchange effect, just making the volume of modern AABW increase, as one might assume from the $\delta^{13}C$ distribution at the LGM, will drive pCO_2 up, as this water mass has high preformed nutrients today [*Hain et al*., 2010]. Upper ocean stratification in the Southern Ocean has been invoked to explain higher nutrient utilization efficiency and lower preformed nutrients in the southern cell at the LGM [*Francois et al*., 1992; *Ren et al*., 2009; *Sigman and Boyle*, 2000], and this should not be confused with the deep stratification discussed above. However, this isolation of the surface from deeper nutrient-rich waters seems to be in conflict with a salty southern sourced deep water at this time as increased sea ice export has been the preferred explanation for the salt, and this requires contact between the deep ocean and the Southern Ocean surface. A new idea for generating salty bottom water from the south that might get around this problem is discussed below.

4.3. A New Idea for How the Deep Ocean Slid Into a Glacial State

[44] Theories for all of the glacial to interglacial deep ocean changes shown in Figure 9 have been presented in the papers reviewed above, but here I combine these basic observations into a relatively simple idea that outlines the deep ocean's role in moving the climate system from an interglacial period to a glacial maximum. As emphasized in the Introduction to this paper, this role must include tracer trapping, specifically CO_2, in the deep ocean during glacial times and tracer release during interglacials. The basic process behind this new idea is that cooling of NADW must lead to saltier AABW and larger density contrasts in the glacial deep ocean (Figure 11).

[45] In the modern ocean, NADW is essentially the precursor to AABW. Around the Antarctic continent relatively small shelf regions provide a platform to make dense waters via wintertime sea ice formation and export. Making sea ice by atmospheric cooling will only lead to saltier ocean waters if the entire sensible heat content of the water column can be exhausted. Each new moment of brine rejection by seawater freezing leads to a temperature inversion that will tend to remelt the newly made sea ice when convection occurs [*Martinson*, 1990]. For this reason, it is the shallow shelf areas around Antarctica that are the most important for deep water

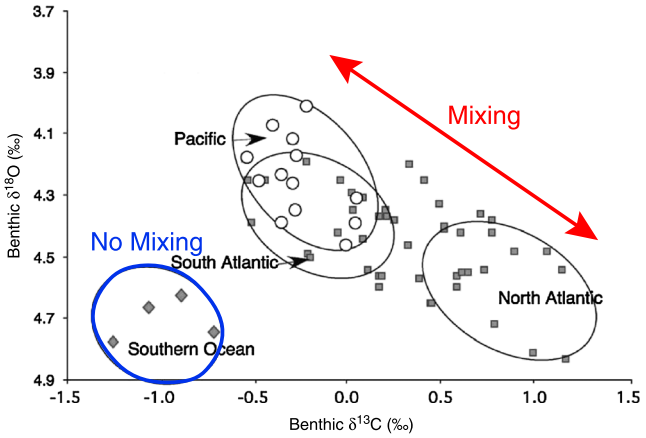

Figure 10. A summary of benthic stable isotope data from the LGM [*Duplessy et al*., 2002] that implies a "two-cell" structure for the deep ocean with little mixing of Southern Source waters. Pore fluid data show that the $\delta^{18}O_w$ values for the deep North Atlantic cores are lower than that for the Pacific core. Combined with the benthic $\delta^{18}O_{CaCO3}$ data in this figure, the data imply that the Pacific must have been warmer than the Atlantic at the LGM. In addition, the benthic data for the Southern Ocean imply that this water does not fall on a mixing line with the other basins. There is a linear trend between the North Atlantic and the Pacific, but the Southern Ocean cores are both heavy in $\delta^{18}O$ and light in $\delta^{13}C$. This is evidence of a two-cell deep circulation at the LGM that is more separated than the modern. It implies that southern sourced water did not mix with northern sourced water at the LGM, but the north, in turn, mixed with a Pacific end-member.

formation. This process leaves saltier waters behind that are dense enough to sink down the continental shelf, entraining ambient waters as they fall to their level of neutral density. The Weddell Sea is the largest of these regions and may contribute up to 50% of the total AABW water mass.

[46] Today the waters that impinge on the Filchner-Ronne ice shelf in the Weddell Sea are modified Circumpolar Deep Waters [*Nicholls et al*., 2009], which are themselves only slightly modified NADW (Figure 11a). As these waters are relatively warm, they melt some of the marine-based continental ice sheet on Antarctica and are cooled to the in situ freezing point. This "prefreshening" is a major component of what makes AABW fresh. In the winter, this fresh water flux is partially compensated for by sea ice formation over the continental shelf, but the end result is cold-fresh AABW. In an annulus model of the ocean around Antarctica, Hellmer studied the effect of removing this prefreshening by building a wall at the front of the ice shelf cavities [*Hellmer*, 2004]. The net result was that cold salty bottom waters were formed around Antarctica that had even larger salinities than their NADW precursor; a result similar to the pore fluid constrained LGM T/S plot for the deep ocean (Figure 7a).

[47] Clearly Hellmer's wall is not a mechanistic description of the LGM, but a colder version of NADW might achieve the same result (Figure 11d). In a new study using a version of the MIT GCM coupled to sea ice and ice shelf cavity models, Miller et al. show that cooling the boundary around the Weddell Sea results in very salty waters forming at the edge of the shelf-slope break [*Miller et al*., 2012]. Due to the lack of well-resolved, or explicitly parameterized, bottom boundary layer processes in the model, these salty waters do not fill the bottom of the Weddell Sea, though their increase in density implies that they should. In this simple model test, cooling NADW leads to salty AABW, or at least a much saltier core of water that would have become AABW if the model's deep convection worked better. This initially counter intuitive result says that if one made NADW cooler today, its density relative to AABW would decrease, even though it seems as if it is NADW's warmth that keeps it from being the most dense water mass in the open ocean. Cooling NADW provides a simple mechanism to establish the cold salty bottom water coming from the Southern Ocean seen in Figure 7a.

[48] With this mechanism in mind, it is possible to see how the deep ocean might evolve into a more effective carbon trap over the course of a glacial cycle. Starting at the previous interglacial (Figures 11a–c), something begins to cool NADW. I hypothesize that this cooling is related to the summertime insolation at 65°N. This cooling leads to less melting of the continental ice around Antarctica and therefore saltier and denser southern source water. As this new water begins to fill the Atlantic, the boundary between northern and southern source waters shoals. Both this shoaling (due to less and less rough topography at the water mass boundary depth) and the new density contrast between water masses lead to lower vertical mixing, which in turn leads to trapping tracer in the southern water mass. During interglacials, the thermobaric effect (the pressure dependence of the thermal expansion coefficient of seawater) assures that the opposing effects of temperature and salinity on the density of the two main deep water masses lead to a smooth density profile with no deep stratification (Figure 11c). As the system transitions into a full glacial, the cold-fresher water in the northern cell no longer finds a natural neutral density level in a smooth transition to AABW because the pressure effect on the haline contraction coefficient is very small. Sinking warmer waters to depth no longer causes a reversal in sign of the north-south density difference. This leads to larger density contrasts between the north and the south and reduced interleaving of the water masses in the vertical profile (Figures 11e and 11f).

[49] It will be difficult to find the north-south deep ocean temperature phasing implied by this idea in sediment core data as the system transitions from interglacial to glacial. The

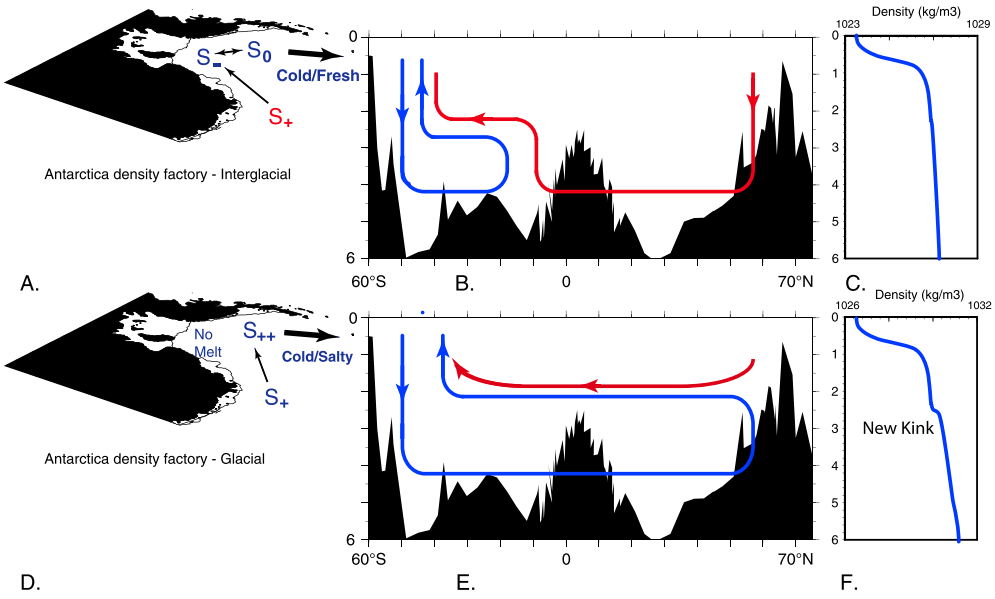

Figure 11. A schematic for the idea that cooling NADW leads to saltier AABW and how this affects the structure of the deep ocean. Figures 11a–c show interglacial states, while Figures 11d–f show the circulation after cooling northern source water leads to saltier and denser southern source water. Following the ideas in *Miller et al.* [2012], Figures 11a and 11d show the Weddell Sea "density factory" as an example of the interplay between NADW temperature and melting of land-based ice. In the modern ocean (a), warm and salty NADW is the bulk of the water that enters the Weddell Sea along the Antarctic margin. The warmth of this water melts some of the land-based ice freshening the waters on the continental shelf (S_-) that are salinified in winter due to sea ice formation (S_0). This wind and sea ice-driven positive salinity flux is not large enough to make up for the freshening from melting the land-based ice, and modern AABW is cold and fresh compared to NADW [*Hellmer*, 2004]. During the LGM (d), and presumably sometime earlier during the glacial, cooler northern source water did not melt as much land ice, but the wind and sea ice-driven salinity flux either increased or stayed the same. Without the prefreshening effect of Antarctic ice melt waters, the salinity contrast between southern and northern sourced waters can switch (S_{++}) as sea ice formation acts to make the newly forming southern waters saltier than the northern sourced input to this system. During interglacials, the opposing effects of salinity and temperature lead to interleaving of NADW and AABW at depth where there is rough topography that enhances the vertical mixing between the two (b). Via the thermobaric effect, warm-salty NADW will always find its neutral density level between the southern sourced water masses and the density profile is smooth with no kinks (c). During glacial periods, cold-salty southern source water is denser than cold-fresh northern source water and the two water masses make contact above the bulk of the deep ocean's rough topography at midocean ridges (e). The thermobaric effect does not play much of a role and mechanically driven vertical mixing from ocean bottom roughness is reduced, each of which gives rise to an extra kink in the density profile (f).

stratigraphic resolution and the errors in temperature estimates are not good enough to resolve the predicted lead of northern cell cooling and southern cell salinification. In addition, we have no good deep ocean salinity tracers that could be used to track this phasing in the first place. However, there are at least two types of data that support this idea. The first data set comes from benthic $\delta^{18}O$ time series. Figure 6 shows several records of deep ocean temperature that were derived from subtracting a sea level component from the raw $\delta^{18}O$ data. It is clear that the entire deep ocean cooled at the MIS 5e to 5d transition ~118,000 years ago. It is also clear that only the Atlantic basin shows a further cooling at the MIS 5/4 transition. From recent high-resolution measurements of pCO_2 across the last glacial cycle, we now know that this 5/4 transition was also a time of ~40 ppmv pCO_2 decrease (Figure 12). While this remarkable correlation between Atlantic deep ocean temperature change and pCO_2 decrease does not prove that the temperature-glacial melting feedback around Antarctica was the cause, it is at least consistent with the idea, and is certainly inconsistent with whole ocean cooling causing the pCO_2 drop at the MIS 5/4 transition. Our hypothesis is that part of the pCO_2 drop at the 5e/5d transition is due to whole ocean cooling, while the signal at the 5/4 transition is due to an increase in stratification of the deep ocean as southern sourced waters become saltier and denser than NADW.

[50] Second, Imbrie et al.'s analysis of dozens of globally distributed sediment cores across many glacial cycles found a clear pattern in the phasing of records at all three Milankovitch frequencies [*Imbrie et al.*, 1992]. In each case, there was a group of cores with an early response and a group with a later response relative to 65°N summer time insolation. All of the Southern Ocean cores were in the early responding group. In the discussion of this paper, Imbrie

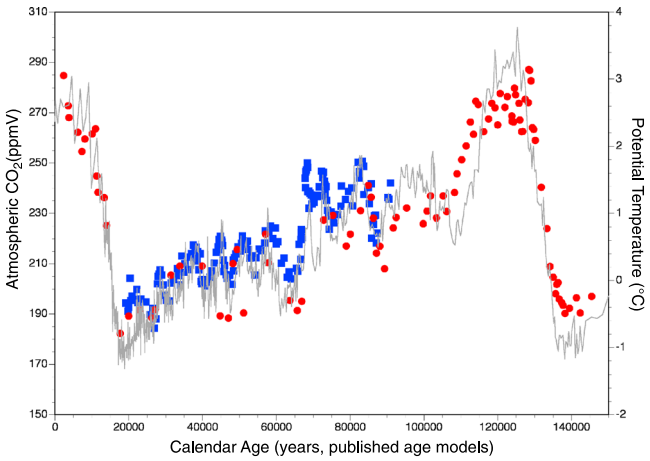

Figure 12. Comparison of deep Atlantic potential temperature (core MD95-2042, gray line) and atmospheric CO_2 from Vostok, red circles [*Petit et al.*, 1999] and blue squares [*Ahn and Brook*, 2008]. Unlike the Pacific record of deep temperature (Figure 6), the Atlantic shows cooling where the CO_2 shows sharp decreases. As the deep ocean is the most important reservoir for setting pCO_2 on these timescales, these data implicate Atlantic processes, as opposed to whole ocean changes, as crucial for CO_2 dynamics, especially at the MIS 5/4 transition.

used the recently published very high resolution record from Troll 3.1 in the North Atlantic to argue that the initiation of glaciation must still have had a Northern Hemisphere origin, though his careful analysis of the data pointed to the Southern Hemisphere (and tropics) instead. The idea that cooling NADW makes AABW saltier can reconcile Imbrie's phasing analysis with a northern forcing because it implies an early response around Antarctica as a result of 65°N summertime forcing. This idea is a candidate for the process that "synchronizes the hemispheres" in glacial-interglacial cycles. An important caveat here is that the Southern Ocean cores in Imbrie's study were mostly from the sub-Antarctic zone, and not directly connected to the polar ocean overturning, where the influence of the circumpolar westerlies might also be of primary importance [*Anderson et al.*, 2009; *Toggweiler et al.*, 2006].

[51] The idea that cooling NADW leads to saltier AABW does not help with the problem of deglaciations. It is not a full theory of glacial-interglacial cycles. If the temperature of northern sourced waters were the only player in glacial cycle dynamics, and if it is linearly related to 65°N summer insolation, then there should be no "sawtooth" character to the records. Some other nonlinearity must be at work in terminations. This idea provides a way to show how Imbrie's phase and coherency analysis, that is only sensitive to glacial buildups because the age models of his cores are not able to constrain differences in terminations, could come about from Milankovitch's presumed forcing. But this idea does not (yet) solve some of the most persistent problems in glacial theory. It is possible that shifts in the winds around Antarctica may have kept the warming northern source water away from the land-based ice until some abrupt change allowed this "hot finger" to melt the ice and reverse the feedback presented here, but this will require more work to examine in detail. What I hope is clear from this idea is that the equation of state (thermobaricity), Milankovitch forcing, and a thermodynamic feedback of warm water melting land-based ice are a set of simple physics that must be at work in the system and that they have important consequences for the structure of the deep ocean circulation.

5. Conclusions

[52] The last glacial maximum deep ocean was characterized by a sharp tracer gradient at ~2000 m water depth in the Atlantic Ocean that represents the boundary between northern sourced and southern sourced deep waters. Mixing across this front was lower than it is today. Along with a saltier source of southern source waters, observations presented here imply that the two deep overturning cells were much less interleaved than they are today. In the Pacific, there is much less data, but the impression is of more radiocarbon-depleted waters at depth but very similar values from the base of the thermocline to at least 2500 m. During the rapid climate changes of the last glacial period, the deep ocean signals are largest during Heinrich events when the distinct two-cell structure in the Atlantic seems to have been interrupted by deep mixing between the water masses. Both the spatial extent and the causes of these events, and what role they might play in deglaciations, are also open questions. It is not clear exactly when this two-cell structure was fully established, but the MIS 5/4 transition is a good candidate. During the slide from the previous interglacial towards the LGM, the whole deep ocean cooled strongly at the 5e/5d transition but the Atlantic shows an additional dramatic cooling at the MIS 5/4 event. These signals are consistent with the record of atmospheric CO_2 over the last glacial cycle and mark the importance of deep ocean water mass structure in setting the pCO_2. The feedback between the temperature of deep waters that impinge on the Antarctic ice sheet and the salinity of newly forming AABW could have led to this salinity stratified LGM deep ocean. In future work, it is important to firmly establish, or not, that the LGM was more stratified than today and that this was supported by salinity contrasts. In addition, a fuller examination of the circulation state before, during, and after the MIS 5/4 transition should

shed important light on how the deep ocean helps set the mean climate during glacial-interglacial cycles.

[53] **Acknowledgments.** This work has greatly benefited from conversations with many people over the years. Ed Boyle and Danny Sigman have taught me much of what I know about the carbonate system, though any mistakes about CO_2 feedbacks in this paper are mine alone. A sabbatical in the CNRS lab at Gif-sur-Yvette provided the time and intellectual space for the initial idea about feedbacks between NADW and AABW formation to germinate into a nascent theory of glacial to interglacial change. I thank them immensely for their hospitality, good humor, and critical ears. My group at Caltech has provided both new ideas and a sounding board for this paper during its long development. Madeline Miller and Andrea Burke are especially thanked for close readings of a fairly complete draft. Two reviewers, Luke Skinner and one anonymous, provided a careful, close, and critical reading of the manuscript that helped improve it greatly. Finally, Chris Charles was an extremely patient editor as well as an important critic of this paper during its several incarnations. I am deeply indebted to him for his help. This work was partially supported by NSF grants OCE 1204211 and OCE 0929272.

References

Adkins, J. F., and E. A. Boyle (1997), Changing atmospheric D14C and the record of paleo-ventilation ages, *Paleoceanography*, *12*, 337–344.

Adkins, J. F., H. Cheng, E. A. Boyle, E. R. M. Druffel, and L. Edwards (1998), Deep-sea coral evidence for rapid change in ventilation of the deep North Atlantic 15,400 years ago, *Science*, *280*, 725–728.

Adkins, J. F., K. McIntyre, and D. P. Schrag (2002a), The salinity, temperature, and d18O of the glacial deep ocean, *Science*, *298*, 69–73.

Adkins, J. F., S. Griffin, M. Kashgarian, H. Cheng, E. R. M. Druffel, E. A. Boyle, R. L. Edwards, and C.-C. Shen (2002b), Radiocarbon dating of deep-sea corals, *Radiocarbon*, *44*, 567–580.

Ahagon, N., K. Ohkushi, M. Uchida, and T. Mishima (2003), Title: Mid-depth circulation in the northwest Pacific during the last deglaciation: Evidence from foraminiferal radiocarbon ages, *Geophys. Res. Lett.*, *30*(21), 2097, doi:10.1029/2003GL018287.

Ahn, J., and E. Brook (2008), Atmospheric CO2 and Climate on Millennial Time Scales During the Last Glacial Period, *Science*, *322*, 83–85.

Alley, R. B., A. J. Gow, S. J. Johnsen, J. Kipfstuhl, D. A. Meese, and T. Thorsteinsson (1995), Comparison of deep ice cores, *Nature*, *373*, 393–394.

Anderson, R. F., S. Ali, L. I. Bradtmiller, S. H. H. Nielsen, M. Q. Fleisher, B. E. Anderson, and L. H. Burckle (2009), Wind-Driven Upwelling in the Southern Ocean and the Deglacial Rise in Atmospheric CO2, *Science*, *323*, 1443–1448.

Arsouze, T., J.-C. Dutay, F. Lacan, and C. Jeandel (2007), Modeling the neodymium isotopic composition with a global ocean circulation model, *Chem. Geol.*, *239*, 165–177.

Arsouze, T., A. M. Treguier, S. Peronne, J.-C. Dutay, F. Lacan, and C. Jeandel (2010), Modeling the Nd isotopic composition in the North Atlantic basin using an eddy-permitting model, *Ocean Sci.*, *6*, 789–797.

Bard, E. (1988), Correction of accelerator mass spectrometry ^{14}C ages measured in planktonic foraminifera: Paleoceanographic implications, *Paleoceanography*, *3*, 635–645.

Bard, E., B. Hamelin, R. G. Fairbanks, and A. Zindler (1990), Calibration of the ^{14}C timescale over 30,000 years using mass spectrometric U-Th ages from Barbados corals, *Nature*, *345*, 405–410.

Barnola, J. M., D. Raynaud, Y. S. Korotkevitch, and C. Lorius (1987), Vostok ice core: a 160,000-year record of atmospheric CO2, *Nature*, *329*, 408–414.

Behl, R. J., and J. P. Kennett (1996), Brief interstadial events in the Santa Barbara basin, NE Pacific, during the past 60 kyr, *Nature*, *379*, 243–246.

Bemis, B. E., H. J. Spero, J. Bijma, and D. W. Lea (1998), Reevaluation of the oxygen isotopic composition of planktonic foraminifera: Experimental results and revised paleotemperature equations, *Paleoceanography*, *13*, 150–160, doi:10.1029/98PA00070.

Blunier, T., and E. Brook (2001), Timing of millennial-scale climate change in Antarctica and Greenland during the last glacial period, *Science*, *291*, 109–112.

Boyle, E. A. (1988), Cadmium: chemical tracer of deepwater paleoceanography, *Paleoceanography*, *3*, 471–489.

Boyle, E. A. (2000), Is the ocean thermohaline circulation linked to abrupt stadial/interstadial transitions?, *Quat. Sci. Rev.*, *19*, 255–272.

Boyle, E. A., and L. D. Keigwin (1982), Deep circulation of the North Atlantic over the last 200,000 years: Geochemical evidence, *Science*, *218*, 784–787.

Boyle, E. A., and L. D. Keigwin (1985/6), Comparison of Atlantic and Pacific paleochemical records for the last 250,000 years: changes in deep ocean circulation and chemical inventories, *Earth Planet. Sci. Lett.*, *76*, 135–150.

Broecker, W. S. (1998), Paleocean circulation during the last deglaciation: A bipolar seasaw?, *Paleoceanography*, *13*, 119–121.

Broecker, W. S., and G. H. Denton (1990), The role of ocean–atmosphere reorganizations in glacial cycles, *Quat. Sci. Rev.*, *9*, 305–341.

Broecker, W. S., and T. H. Peng (1987), The role of CaCO3 compensation in the glacial to interglacial CO2 change, *Global Biogeochem. Cycles*, *1*, 15–30.

Broecker, W. S., and J. van Donk (1970), Insolation Changes, Ice Volumes, and the O18 Record in Deep-Sea Cores, *Rev. Geophys. Space Phys.*, *8*, 169–198.

Broecker, W. S., M. Andree, G. Bonani, W. Wolfli, H. Oeschger, M. Klas, and W. Curry (1988), Preliminary estimates for the radiocarbon age of deep water in the glacial ocean, *Paleoceanography*, *3*, 659–669.

Broecker, W. S., T. H. Peng, S. Trumbore, G. Bonani, and W. Wolfli (1990a), The distribution of radiocarbon in the glacial ocean, *Global Biogeochem. Cycles*, *4*, 103–117.

Broecker, W. S., G. Bond, M. Klas, G. Bonani, and W. Wolfli (1990b), A salt oscillator in the glacial northern Atlantic? 1 The concept, *Paleoceanography*, *5*, 469–477.

Broecker, W. S., S. Sutherland, W. Smethie, T.-H. Peng, and G. Ostlund (1995), Oceanic radiocarbon: Separation of the natural and bomb components, *Global Biogeochem. Cycles*, *9*, 263–288.

Broecker, W. S., K. Matsumoto, E. Clark, I. Hajdas, and G. Bonani (1999), Radiocarbon age differences between coexisting foraminiferal species, *Paleoceanography*, *14*, 431–436.

Broecker, W. S., S. Barker, E. Clark, I. Hajdas, G. Bonani, and L. Stott (2004), Ventilation of the glacial deep Pacific Ocean, *Science*, *306*, 1169–1172.

Broecker, W. S., S. Barker, E. Clark, I. Hajdas, and G. Bonani (2006), Anomalous radocarbon ages for foraminifera shells, *Paleoceanography*, *21*, PA2008, doi:10.1029/2005PA001212.

Bryan, S., and T. M. Marchitto (2008), Mg/Ca-temperature proxy in benthic foraminifera: New calibrations from the Florida Straits and a hypothesis regarding Mg/Li, *Paleoceanography*, *23*, PA2220, doi:10.1029/2007PA001553.

Bryan, S., T. M. Marchitto, and S. Lehman (2010), The release of 14C-depleted carbon from the deep ocean during the last deglaciation: Evidence from the Arabian Sea, *Earth Planet. Sci. Lett.*, *4*, 244–254.

Burke, A., and L. F. Robinson (2012), The Southern Ocean's Role in Carbon Exchange During the Last Deglaciation, *Science*, *335*, 557–561.

Burke, A., O. Marchal, L. I. Bradtmiller, J. F. McManus, and R. François (2011), Application of an inverse method to interpret 231Pa/230Th observations from marine sediments, *Paleoceanography*, *26*, PA1212, doi:10.1029/2010PA002022.

Caillon, N., J. Severinghaus, J. Jouzel, J.-M. Barnola, J. Kang, and V. Lipenkov (2003), Timing of Atmospheric CO2 and Antarctic Temperature Changes Across Termination III, *Science*, *299*, 1728–1731.

Came, R., D. W. Oppo, and W. B. Curry (2003), Atlantic Ocean circulation during the Younger Dryas: Insights from a new Cd/Ca record from the Western subtropical South Pacific, *Paleoceanography*, *18*(4), 1086, doi:10.1029/2003PA000888.

Case, D., L. Robinson, M. Auro, and A. Gagnon (2010), Environmental and biological controls on Mg and Li in deep-sea scleractinian corals, *Earth Planet. Sci. Lett.*, *300*, 215–225.

Chappell, J., and N. J. Shackleton (1986), Oxygen isotopes and sea level, *Nature*, *324*, 137–140.

Charles, C. D., and R. G. Faibanks (1992), Evidence from Southern Ocean sediments for the effect of North Atlantic deep-water flux on climate, *Nature*, *355*, 416–419.

Charles, C., J. D. Wright, and R. Fairbanks (1993), Thermodynamic influences on the marine carbon isotope record, *Paleoceanography*, *8*, 691–697.

Charles, C. D., J. Lynch-Stieglitz, U. S. Ninnemann, and R. G. Fairbanks (1996), Climate connections between the hemisphere revealed by deep sea sediment core/ice core correlations, *Earth Planet. Sci. Lett.*, *142*, 19–27.

Crowley, T. (1992), North Atlantic Deep Water Cools the Southern Hemisphere, *Paleoceanography*, *7*, 489–497.

Curry, W., and G. P. Lohmann (1983), Reduced advection into Atlantic Ocean deep eastern basins during last glaciation maximum, *Nature*, *306*, 577–580.

Curry, W. B., and D. W. Oppo (1997), Synchronous, high-frequency oscillations in tropical sea surface temperatures and North Atlantic Deep Water production during the last glacial cycle, *Paleoceanography*, *12*, 1–14.

Curry, W. B., and D. Oppo (2005), Glacial Water Mass Geometry and the Distribution of d13C of Total CO2 in the Western Atlantic Ocean, *Paleoceanography*, *20*, PA1017, doi:10.1029/2004PA001021.

Cutler, K. B., R. L. Edwards, F. W. Taylor, H. Cheng, J. Adkins, C. D. Gallup, P. M. Cutler, G. S. Burr, J. Chappell, and A. L. Bloom (2003), Rapid sea-level fall and deep-ocean temperature change since the last interglacial, *Earth Planet. Sci. Lett.*, *206*, 253–271.

Dansgaard, W., and H. Tauber (1969), Glacier oxygen-18 content and Pleistocene ocean temperatures, *Science*, *166*, 499–502.

Dansgaard, W., et al. (1993), Evidence of general instability of past climate from a 250-kyr ice-core record, *Nature*, *364*, 218–220.

De Pol-Holz, R., L. Keigwin, J. Southon, D. Hebbeln, and M. Mohtadi (2011), No signature of abyssal carbon in intermediate waters off Chile during deglaciation, *Nat. Geosci.*, *3*, 192–195.

DeVries, T., and F. Primeau (2011), Dynamically and Observationally Constrained Estimates of Water-Mass Distributions and Ages in the Global Ocean, *J. Phys. Oceanogr.*, *41*, 2381–2401.

Duplessy, J.-C., N. J. Shackleton, R. G. Fairbanks, L. Labeyrie, D. Oppo, and N. Kallel (1988), Deep water source variations during the last climatic cycle and their impact on the global deep water circulation, *Paleoceanography*, *3*, 343–360.

Duplessy, J. C., C. Lalou, and A. C. Vinot (1970), Differential isotopic fractionation in benthic foraminifera and paleotemperatures re-assessed, *Science*, *168*, 250–251.

Duplessy, J. C., R. K. Matthews, W. Prell, W. F. Ruddiman, M. Caralp, and C. H. Hendy (1984), 13C record of benthic forminifera in the last interglacial ocean: implications for the carbon cycle and global deep water circulation, *Quat. Res.*, *21*, 225–243.

Duplessy, J.-C., M. Arnold, E. Bard, A. Juillet-Leclerc, N. Kallel, and L. Labeyrie (1989), AMS 14C study of transient events and of the ventilation rate of the Pacific intermediate water during the last deglaciation, *Radiocarbon*, *31*, 493–502.

Duplessy, J.-C., L. Labeyrie, and C. Waelbroeck (2002), Constraints on the ocean oxygen isotopic enrichment between the Last Glacial Maximum and the Holocene: paleoceanographic implications, *Quat. Sci. Rev.*, *21*, 315–330.

Edwards, L. R., W. J. Beck, G. S. Burr, D. J. Donahue, J. M. A. Chappell, A. L. Bloom, E. R. M. Druffel, and F. W. Taylor (1993), A large drop in atmospheric $^{14}C/^{12}C$ and reduced melting in the Younger Dryas, documented with ^{230}Th ages of corals, *Science*, *260*, 962–8.

Eiler, J. M. (2011), Paleoclimate reconstruction using carbonate clumped isotope thermometry, *Quat. Sci. Rev.*, *30*, 3575–3588.

Elderfield, H., and G. Ganssen (2000), Past temperature and delta O-18 of surface ocean waters inferred from foraminiferal Mg/Ca ratios, *Nature*, *405*, 442–445.

Elderfield, H., P. Ferretti, M. Greaves, S. Crowhurst, I. McCave, D. Hodell, and A. M. Piotrowski (2012), Evolution of ocean temperature and ice volume through the Mid-Pleistocene climate transition, *Science*, *337*, 704–709.

Elmore, A. C., A. M. Piotrowski, J. D. Wright, and A. E. Scrivner (2011), Testing the extraction of past seawater Nd isotopic composition from North Atlantic deep sea sediments and foraminifera, *Geochem. Geophys. Geosyst.*, *12*, Q09008, doi:10.1029/2011GC003741.

Eltgroth, S. F., J. F. Adkins, L. Robinson, J. Southon, and M. Kashgarian (2006), A deep-sea coral record of North Atlantic radiocarbon through the Younger Dryas: Evidence for Intermediate/Deep water reorganization, *Paleoceanography*, *21*, PA4207, doi:10.1029/2005PA001192.

Emile-Geay, J., and G. Madec (2009), Geothermal heating, diapycnal mixing and the abyssal circulation, *Ocean Sci.*, *5*, 203–217.

Emiliani, C. (1966), Paleotemperature analysis of Caribbean cores P 6304–8 and P 6304–9 and a generalised temperature curve for the last 425,000 years, *J. Geol.*, *74*, 109–124.

EPICA (2004), Eight glacial cycles from an Antarctic ice core, *Nature*, *429*, 623–628.

Erez, J. (1978), Vital effect on stable-isotope composition seen in foraminifera and coral skeletons, *Nature*, *273*, 199–202.

Erez, J. (2003), The sources of ions for biomineralization in foraminifera and their implications for paleoceanographic proxies, in *Reviews in Mineralogy and Geochemistry: Biomineralization*, vol. 54, edited by P. M. Dove, J. J. D. Yoreo, and S. Weiner, pp. 115–149, Mineralogical Society of America, Washington, DC.

Evans, H. K., I. Hall, G. G. Bianchi, and D. W. Oppo (2007), Intermediate water links to Deep Western Boundary Current variability in the subtropical NWAtlantic during marine isotope stages 5 and 4, *Paleoceanography*, *22*, PA3209, doi:10.1029/2006PA001409.

Ferrari, R., and C. Wunsch (2009), Ocean Circulation Kinetic Energy: Reservoirs, Sources, and Sinks, *Annu. Rev. Fluid Mech.*, *41*, 253–282.

Francois, R., M. A. Altabet, and L. H. Burckle (1992), Glacial to interglacial changes in surface nitrate utillization in the Indian sector of the Southern Ocean as recorded by sediment d15N, *Paleoceanography*, *7*, 589–606.

Galbraith, E. D., S. L. Jaccard, T. F. Pedersen, D. Sigman, G. H. Haug, M. Cook, J. Southon, and R. Francois (2007), Carbon dioxide release from the North Pacific abyss during the last deglaciation, *Nature*, *449*, 890–893.

Ganachaud, A., and C. Wunsch (2000), Improved estimates of global ocean circulation, heat transport and mixing from hydrographic data, *Nature*, *408*, 453–457.

Gebbie, G. (2012), Tracer transport timescales and the observed Atlantic-Pacific lag in the timing of the Last Termination, *Paleoceanography*, *27*, PA3225, doi:10.1029/2011PA002273.

Gebbie, G., and P. Huybers (2010), Total Matrix Intercomparison: A Method for Determining the Geometry of Water-Mass Pathways, *J. Phys. Oceanogr.*, *40*, 1710–1728.

Gherardi, J.-M., L. Labeyrie, J. McManus, R. Francois, L. Skinner, and E. Cortijo (2005), Evidence from the Northeastern Atlantic basin for variability in the rate of the meridional overturning circulation through the last deglaciation, *Earth Planet. Sci. Lett.*, *240*, 710–723.

Gherardi, J.-M., L. Labeyrie, S. Nave, R. Francois, J. F. McManus, and E. Cortijo (2009), Glacial-interglacial circulation changes inferred from 231Pa/230Th sedimentary record in the North Atlantic region, *Paleoceanography*, *24*, PA2204, doi:10.1029/2008PA001696.

Ghosh, P., J. F. Adkins, H. Affek, B. Balta, W. Guo, E. A. Schauble, D. P. Schrag, and J. M. Eiler (2006), 13C-18O bonds in carbonate minerals: A new kind of paleothermometer, *Geochim. Cosmochim. Acta*, *70*, 1439–1456.

Gildor, H., and E. Tziperman (2003), Sea-ice switches and abrupt climate change, *Philos. Trans. R. Soc. London*, *361*, 1935–1942.

Goldstein, S. J., D. W. Lea, S. Chakraborty, M. Kashgarian, and M. T. Murrell (2001), Uranium-series and radiocarbon geochronology of deep-sea corals: implications for Southern Ocean ventilation rates and the oceanic carbon cycle, *Earth Planet. Sci. Lett.*, *193*, 167–182.

GRIP (1993), Climate instability during the last interglacial period recorded in the GRIP ice core, *Nature*, *364*, 203–207.

Grootes, P. M., M. Stuiver, J. W. C. White, S. Johnsen, and J. Jouzel (1993), Comparison of oxygen isotope records from GISP2 and GRIP Greenland ice cores, *Nature*, *366*, 552–554.

Hain, M., D. M. Sigman, and G. H. Haug (2010), Carbon dioxide effects of Antarctic stratification, North Atlantic Intermediate Water formation, and subantarctic nutrient drawdown during the last ice age: Diagnosis and synthesis in a geochemical box model, *Global Biogeochem. Cycles*, *24*, GB4023, doi:10.1029/2010GB003790.

Hain, M., D. Sigman, and G. H. Haug (2011), Shortcomings of the isolated abyssal reservoir model for deglacial radiocarbon changes in the mid-depth Indo-Pacific Ocean, *Geophys. Res. Lett.*, *38*, L04604, doi:10.1029/2010GL046158.

Hall, T. M., and T. W. N. Haine (2002), On ocean transport diagnostics: The idealized age tracer and the age spectrum, *J. Phys. Oceanogr.*, *32*, 1987–1991.

Hall, I., and I. McCave (2000), Palaeocurrent reconstruction, sediment and thorium focussing on the Iberian margin over the last 140 ka, *Earth Planet. Sci. Lett.*, *178*, 151–164.

Headly, M., and J. Severinghaus (2007), A method to measure Kr/N-2 ratios in air bubbles trapped in ice cores and its application in reconstructing past mean ocean temperature, *J. Geophys. Res.*, *112*, D19105, 10.1029/2006JD008317.

Heinrich, H. (1988), Origin and consequences of cyclic ice rafting in the northeast Atlantic Ocean during the past 130,000 years, *Quat. Res.*, *29*, 142–152.

Hellmer, H. H. (2004), Impact of Antarctic ice shelf basal melting on sea ice and deep ocean properties, *Geophys. Res. Lett.*, *31*, L10307, doi:10.1029/2004GL019506.

Hemming, S. R. (2004), Heinrich events: Massive late Pleistocene detritus layers of the North Atlantic and their global climate imprint, *Rev. Geophys.*, *42*, RG1005, doi:10.1029/2003RG000128.

Hodell, D. A., K. A. Venz, C. D. Charles, and U. S. Ninnemann (2003), Pleistocene vertical carbon isotope and carbonate gradients in the South Atlantic sector of the Southern Ocean, *Geochem. Geophys. Geosyst.*, *4*(1), 1004, doi:10.1029/2002GC000367.

Hönisch, B., J. Bijma, A. D. Russell, H. J. Spero, M. R. Palmer, R. E. Zeebe, and A. Eisenhauer (2003), The influence of symbiont photosynthesis on the boron isotopic composition of foraminifera shells, *Mar. Micropaleontol.*, *49*, 87–96.

Hönisch, B., N. G. Hemming, D. Archer, M. Siddall, and J. F. McManus (2009), Atmospheric Carbon Dioxide Concentration over the Mid Pleistocene Transition, *Science*, *324*, 1551–1554.

Huybers, P., G. Gebbie, and O. Marchal (2007), Can Paleoceanographic Tracers Constrain Meridional Circulation Rates?, *J. Phys. Oceanogr.*, *37*, 394–407.

Imbrie, J., et al. (1992), On the structure and origin of major glaciation cycles: 1 Linear responses to Milankovitch forcing, *Paleoceanography*, *7*, 701–738.

Ingram, B. L., and J. P. Kennett (1995), Radiocarbon chronology and planktonic-benthic foraminiferal 14C age differences in Santa Barbara basin sediments, Hole 893A, Procedings of the Ocean Drilling Program, 146 (pt.2), 19–27.

Jackett, D. R., and T. McDougall (1997), A Neutral Density Variable for the World's Oceans, *J. Phys. Oceanogr.*, *27*, 237–263.

Johnson, G. C. (2008), Quantifying Antarctic Bottom Water and North Atlantic Deep Water volumes, *J. Geophys. Res.*, *113*, C05027, doi:10.1029/2007JC004477.

Joyce, T. M., B. A. Warren, and L. D. TAlley (1986), The geothermal heating of the abyssal subarctic Pacific Ocean, *Deep-Sea Res.*, *33*, 1003–1015.

Kallel, N., L. D. Labeyrie, A. Juillet-Laclerc, and J. C. Duplessy (1988), A deep hydrological front between intermediate and deep water masses in the glacial Indian Ocean, *Nature*, *333*, 651–655.

Keigwin, L. (2004), Radiocarbon and stable isotope constraints on Last Glacial Maximum and Younger Dryas ventilation in the Western North Atlantic, *Paleoceanography*, *19*, PA4012, doi:10.1029/2004PA001029.

Keigwin, L., and E. A. Boyle (2008), Did North Atlantic overturning halt 17,000 years ago?, *Paleoceanography*, *23*, PA1101, doi:10.1029/2007PA001500.

Keigwin, L., and M. Schlegel (2002), Ocean ventilation and sedimentation since the glacial maximum at 3 km in the western North Atlantic, *Geochem. Geophys. Geosyst.*, *3*(6), 1034, doi:10.1029/2001GC000283.

Keigwin, L., M. L. Bender, and J. P. Kennett (1979), Thermal Structure of the Deep Pacific Ocean in the Early Pliocene, *Science*, *205*, 1386–1388.

Knox, F., and M. McElroy (1984), Changes in atmospheric CO2: influence of biota at high latitudes, *J. Geophys. Res.*, *89*, 4629–4637.

Kroopnick, P. M. (1985), The distribution of C-13 in the world oceans, *Deep Sea Res.*, *32*, 57–84.

Labeyrie, L. D., J. C. Duplessy, and P. L. Blanc (1987), Variations in mode of formation and temperature of oceanic deep waters over the past 125,000 years, *Nature*, *327*, 477–482.

Lacan, F., and C. Jeandel (2005), Neodymium isotopes as a new tool for quantifying exchange fluxes at the continent-ocean interface, *Earth Planet. Sci. Lett.*, *232*, 245–257.

Lacan, F., K. Tachikawa, and C. Jeandel (2012), Neodymium isotopic composition of the oceans: A compilation of seawater data, *Chem. Geol.*, *300–301*, 177–184.

Lea, D. W. (1995), A trace metal perspective on the evolution of AntarcticCircumpolar Deep Water chemistry, *Paleoceanography*, *10*, 743–747.

Lea, D., and E. Boyle (1989), Barium content of benthic foraminifera controlled by bottom water composition, *Nature*, *338*, 751–753.

Lea, D. W., and E. A. Boyle (1990), A 210,000-year record of barium variability in the deep northwest Atlantic Ocean, *Nature*, *347*, 269–272.

Lea, D., P. M. Martin, D. Pak, and H. J. Spero (2002), Reconstructing a 350 ky history of sea level using planktonic Mg/Ca and oxygen isotope records from a Cocos Ridge core, *Quat. Sci. Rev.*, *21*, 283–293.

LeGrand, P., and C. Wunsch (1995), Constraints from paleotracer data on the North Atlantic circulation during the last glacial maximum, *Paleoceanography*, *10*, 1011–1045.

LeGrande, A. N., and G. A. Schmidt (2006), Global gridded data set of the oxygen isotopic composition in seawater, *Geophys. Res. Lett.*, *33*, L12604, doi:10.1029/2006GL026011.

Lund, D., J. F. Adkins, and R. Ferrari (2011a), Abyssal Atlantic circulation during the Last Glacial Maximum: Constraining the ratio between transport and vertical mixing, *Paleoceanography*, *26*, PA1213, doi:10.1029/2010PA001938.

Lund, D., A. Mix, and J. Southon (2011b), Increased ventilation age of the deep northeast Pacific Ocean during the last deglaciation, *Nat. Geosci.*, *4*, 771–774.

Lynch-Stieglitz, J., T. F. Stocker, W. Broecker, and R. Fairbanks (1995), The influence of air-sea exchange on the isotopic composition of oceanic carbon: Observations and modeling, *Global Biogeochem. Cycles*, *9*, 653–665.

Lynch-Stieglitz, J., W. B. Curry, and N. Slowey (1999a), Weaker Gulf Stream in the Florida Straits during the Last Glacial Maximum, *Nature*, *402*, 644–648.

Lynch-Stieglitz, J., W. B. Curry, and N. Slowey (1999b), A geostrophic transport estimate for the Florida Current from the oxygen isotope composition of benthic foraminifera, *Paleoceanography*, *14*, 360–373.

Lynch-Stieglitz, J., W. B. Curry, D. W. Oppo, U. Ninnemann, C. Charles, and J. Munson (2006), Meridional overturning circulation in the South Atlantic at the last glacial maximum, *Geochem. Geophys. Geosyst.*, *7*, Q10N03, doi:10.1029/2005GC001226.

Lynch-Stieglitz, J., M. Schmidt, and W. B. Curry (2011), Evidence from the Florida Straits for Younger Dryas ocean circulation changes, *Paleoceanography*, *26*, PA1205, doi:10.1029/2010PA002032.

Mangini, A., M. Lomitschka, R. Eichstadter, N. Frank, S. Vogler, G. Bonani, I. Hajdas, and J. Patzold (1998), Coral provides way to age deep water, *Nature*, *392*, 347–348.

Mangini, A., J. M. Godoy, M. L. Godoy, R. Kowsmann, G. Santos, M. Ruckelshausen, A. Schroeder-Ritzrau, and L. Wacker (2010), Deep sea corals off Brazil verify a poorly ventilated Southern Pacific Ocean during H2, H1 and the Younger Dryas, *Earth Planet. Sci. Lett.*, *293*, 269–276.

Manighetti, B., and I. McCave (1995), Late glacial and Holocene palaeocurrents around Rockall Bank, NE Atlantic Ocean, *Paleoceanography*, *10*, 611–626.

Marchal, O., and W. Curry (2008), On the Abyssal Circulation in the Glacial Atlantic, *J. Phys. Oceanogr.*, *38*, 2014–2037.

Marchal, O., R. Francois, T. F. Stocker, and F. Joos (2000), Ocean thermohaline circulation and sedimentary Pa/Th ratio, *Paleoceanography*, *15*, 625–641.

Marchitto, T. M., and W. Broecker (2006), Deep water mass geometry in the glacial Atlantic Ocean: A review of constraints from the paleonutrient proxy Cd/Ca, *Geochem. Geophys. Geosyst.*, *7*, Q12003, doi:10.1029/2006GC001323.

Marchitto, T. M., W. B. Curry, and D. W. Oppo (1998), Millennial-scale changes in North Atlantic circulation since the last glaciation, *Nature*, *393*, 557–561.

Marchitto, T. M., W. B. Curry, and D. W. Oppo (2000), Zinc concentrations in benthic foraminifera reflect seawater chemistry, *Paleoceanography*, *15*, 299–306.

Marchitto, T. M., S. Lehman, J. Ortiz, J. Fluckiger, and A. vanGeen (2007), Marine radiocarbon evidence for the Mechanism of deglacial atmospheric CO2 rise, *Science*, *316*, 1456–1459.

Martin, E. E., and H. D. Scher (2004), Preservation of seawater Sr and Nd isotopes in fossil fish teeth: bad news and good news, *Earth Planet. Sci. Lett.*, *220*(1–2), 25–39.

Martin, P. M., D. W. Lea, Y. Rosenthal, T. P. Papenfuss, and M. Sarnthein (1998), Late Quaternary deep sea temperatures inferred from benthic foraminiferal Magnesium, paper presented at AGU.

Martin, P. M., D. E. Archer, and D. W. Lea (2005), Role of deep sea temperature in the carbon cycle during the last glacial, *Paleoceanography*, *20*, PA2015, doi:10.1029/2003PA000914.

Martinson, D. G. (1990), Evolution of the Southern Ocean winter mixed layer and sea ice: open ocean deepwater formation and ventilation, *J. Geophys. Res.*, *95*, 11,641–11,654.

McCave, I., and I. Hall (2006), Size sorting in mairne muds: Processes, pitfalls, and prospects for paleoflow-speed proxies, *Geochem. Geophys. Geosyst.*, *7*, Q10N05, doi:10.1029/2006GC001284.

McCave, I., B. Manighetti, and N. Beveridge (1995), Circulation in the Glacial North Atlantic Inferred from Grain-Size Measurements, *Nature*, *374*, 149–152.

McDuff, R. E. (1985), The chemistry of interstitial waters, deep sea drilling project leg 86, in *Init. Rept. of the DSDP*, vol. 86, edited by G. R. Heath et al., pp. 675–687, U.S. Govt. Printing Office, Washington.

McManus, J., R. Francois, J. Gherardi, L. Keigwin, and S. Brown-Leger (2004), Collapse and rapid resumption of Atlantic meridional circulation linked to deglacial climate changes, *Nature*, *428*, 834–837.

Miller, M., J. F. Adkins, D. Menemenlis, and M. P. Schodlok (2012), The role of ice shelves in setting glacial ocean bottom water salinity, *Paleoceanography*, *27*, PA3207, doi:10.1029/2012PA002297.

Munk, W. (1966), Abyssal Recipies, *Deep-Sea Res.*, *13*, 707–730.

Neftel, A., E. Moor, H. Oeschger, and B. Stauffer (1985), Evidence from polar ice cores for the increase in atmospheric CO2 in the past two centuries, *Nature*, *315*, 45–47.

Nicholls, K., S. Østerhus, K. Makinson, T. Gammelsrød, and E. Fahrbach (2009), Ice-ocean processes over the continental shelf of the southern Weddell Sea, *Rev. Geophys.*, *47*, RG3003, doi:10.1029/2007RG000250.

Ninnemann, U., and C. D. Charles (2002), Changes in the mode of Southern Ocean circulation over the last glacial cycle revealed by foraminiferal stable isotopic variability, *Earth Planet. Sci. Lett.*, *201*, 383–396.

Oppo, D., and R. G. Fairbanks (1987), Variability in the deep and intermediate water circulation of the Atlantic Ocean during the past 25,000 years: Northern hemisphere modulation of the Southern Ocean, *Earth Planet. Sci. Lett.*, *86*, 1–15.

Oppo, D., and M. Horowitz (2000), Glacial deep water geometry: South Atlantic benthic foraminiferal Cd/Ca and delta C-13 evidence, *Paleoceanography*, *15*, 147–160.

Otto-Bliesner, B., C. D. Hewitt, T. M. Marchitto, E. Brady, A. Abe-Ouchi, M. Crucifix, S. Murakami, and S. L. Weber (2007), Last glacial maximum ocean thermohaline circulation: PIMP2 model intercomparisons and data contraints, *Geophys. Res. Lett.*, *34*, L12706,doi:10.1029/2007GL029475.

Petit, J.-R., et al. (1999), Climate and atmospheric history of the past 420,000 years from the Vostok ice core, Antarctica, *Nature*, *399*, 429–436.

Piotrowski, A. M., S. J. Goldstein, S. R. Hemming, and R. Fairbanks (2005), Temporal relationships of carbon cycling and ocean circulation at glacial boundaries, *Science*, *307*, 1933–1938.

Polzin, K. L., J. M. Toole, J. R. Ledwell, and R. W. Schmitt (1997), Spatial variability of turbulent mixing in the abyssal ocean, *Science*, *276*, 93–96.

Rae, J., G. Forster, D. Schmidt, and T. R. Elliot (2011), Boron isotopes and B/Ca in benthic foraminifera: Proxies for the deep ocean carbonate system, *Earth Planet. Sci. Lett.*, *302*, 403–413.

Reid, J. L. (1981), On the mid-depth circulation of the world ocean, in *Evolution of physical oceanography*, edited by B. A. Warren and C. Wunsch, pp. 70–111, MIT Press, Cambridge, MA.

Ren, H., D. M. Sigman, A. N. Meckler, B. Plessen, R. S. Robinson, Y. Rosenthal, and G. H. Haug (2009), Foraminiferal isotope evidence of reduced nitrogen fixation in the ice age Atlantic Ocean, *Science*, *323*, 244–248.

Rickaby, R. E. M., and H. Elderfield (2005), Evidence from the high-latitude North Atlantic for variations in Antarctic Intermediate water flow during the last deglaciation, *Geochem. Geophys. Geosyst.*, *6*, Q05001, doi:10.1029/2004GC000858.

Rintoul, S. R., C. W. Hughes, and D. Olbers (2001), The Antarctic circumpolar current system, in *Ocean Circulation and Climate*, edited by G. Siedler, pp. 271–302, Academic Press, London.

Ritz, S., T. Stocker, and J. Severinghaus (2011), Noble gases as proxies of mean ocean temperature: sensitivity studies using a climate model of reduced complexity, *Quat. Sci. Rev.*, *30*(25–26), 3728–3741.

Robinson, L. F., and T. van de Flierdt (2009), Southern Ocean evidence for reduced export of North Atlantic Deep Water during Heinrich event 1, *Geology*, *37*(3), 195–198.

Robinson, L., J. F. Adkins, L. D. Keigwin, J. Southon, D. P. Fernandez, S.-L. Wang, and D. S. Scheirer (2005), Radiocarbon variability in the Western North Atlantic during the last deglaciation, *Science*, *310*, 1469–1473.

Rosenthal, Y., G. P. Lohmann, K. C. Lohmann, and R. M. Sherell (2000), Incorporation and preservation of Mg in Globigerinoides sacculifer: Implications for reconstructing the temperature and 18O/16O of seawater, *Paleoceanography*, *15*, 135–145.

Ruddiman, W. F., B. Molfino, A. Esmay, and E. Pokras (1980), Evidence bearing on the mechanism of rapid deglaciation, *Clim. Change*, *3*, 65–87.

Rutberg, R., S. R. Hemming, and S. J. Goldstein (2000), Reduced North Atlantic Deep Water flux to the glacial Southern Ocean inferred from neodymiumisotope ratios, *Nature*, *405*, 935–938.

Sanyal, A., N. G. Hemming, G. N. Hanson, and W. S. Broecker (1995), Evidence for a higher pH in the glacial ocean from boron isotopes in foraminifera, *Nature*, *373*, 234–236.

Sanyal, A., N. G. Hemming, W. S. Broecker, D. W. Lea, H. J. Spero, and G. N. Hanson (1996), Oceanic pH control on the boron isotopic composition of foraminifera: Evidence from culture experiments, *Paleoceanography*, *11*, 513–517.

Sarmiento, J. L., and J. R. Toggweiler (1984), A new model for the role of the oceans in determining atmospheric pCO2, *Nature*, *308*, 621–624.

Sarnthein, M., K. Winn, S. J. A. Jung, J.-C. Duplessy, L. Labeyrie, H. Erlenkeuser, and G. Ganssen (1994), Changes in east Atlantic deepwater circulation over the last 30,000 years: Eight time slice reconstructions, *Paleoceanography*, *9*, 209–268.

Schlitzer, R. (2002), Carbon export fluxes in the Southern Ocean: results from inverse modeling and comparison with satellite-based estimates, *Deep-Sea Res.*, *49*, 1623–1644.

Schrag, D. P., and D. J. DePaolo (1993), Determination of del18O of seawater in the deep ocean during the Last Glacial Maximum, *Paleoceanography*, *8*, 1–6.

Schrag, D. P., G. Hampt, and D. W. Murry (1996), Pore fluid constraints on the temperature and oxygen isotopic composition of the Glacial ocean, *Science*, *272*, 1930–1932.

Schrag, D. P., J. F. Adkins, K. McIntyre, J. Alexander, D. A. Hodell, C. D. Charles, and J. F. McManus (2002), The Oxygen isotopic composition of seawater during the Last Glacial Maximum, *Quat. Sci. Rev.*, *21*, 331–342.

Schulz, H., U. von Rad, and H. Erlenkeuser (1998), Correlation between Arabian Sea and Geenland climate oscillations of the past 110,000 years, *Nature*, *393*, 54–57.

Shackleton, N. J. (1967), Oxygen isotope analyses and Pleistocene temperatures re-assessed, *Nature*, *215*, 15–17.

Shackleton, N. J. (2000), The 100,000-year ice-age cycle identified and found to lag temperature, carbon dioxide and orbital eccentricity, *Science*, *289*, 1897–1902.

Shackleton, N. J., M. A. Hall, J. Line, and C. Shuxi (1983), Carbon Isotope data in core V19-30 confirm reduced carbon dioxide concentration in the ice age atmosphere, *Nature*, *306*, 319–322.

Shackleton, N. J., J.-C. Duplessy, M. Arnold, P. Maurice, M. A. Hall, and J. Cartlidge (1988), Radiocarbon age of the last glacial Pacific deep water, *Nature*, *335*, 708–711.

Shackleton, N. J., M. A. Hall, and E. Vincent (2000), Phase relationships between millennial-scale events 64,000-24,000 years ago, *Paleoceanography*, *15*, 565–569.

Siani, G., M. Paterne, E. Miche, R. Sulpizio, A. Sbrana, M. Arnold, and G. Haddad (2001), Mediterranean Sea surface radiocarbon reservoir age changes since the last glacial maximum, *Science*, *294*, 1917–1920.

Siegenthaler, U., and T. Wenk (1984), Rapid atmospheric CO2 variations and ocean circulation, *Nature*, *308*, 624–625.

Sigman, D., and E. A. Boyle (2000), Glacial/Interglacial variations in atmospheric carbon dioxide, *Nature*, *407*, 859–869.

Sigman, D. M., S. Lehman, and D. W. Oppo (2003), Evaluating mechanisms of nutrient depletion and 13C enrichment in the intermediate-depth Atlantic during the last ice age, *Paleoceanography*, *18*(3), 1072, doi:10.1029/2002PA000818.

Sigman, D., M. Hain, and G. H. Haug (2010), The polar ocean and glacial cycles in atmospheric CO2 concentration, *Nature*, *466*, 47–55.

Sikes, E., C. Samson, T. Guilderson, and W. Howard (2000), Old radiocarbon ages in the southwest Pacific Ocean during the last glacial period and deglaciation, *Nature*, *405*, 555–559.

Skinner, L. (2009), Glacial-interglacial atmospheric CO2 change: A possilble 'standing volume' effect on deep-ocean carbon sequestration, *Clim. Past*, *5*, 537–550.

Skinner, L., and H. Elderfield (2007), Rapid fluctuations in the deep North Atlantic heat budget during the last glacial period, *Paleoceanography*, *22*, PA1205, doi:10.1029/2006PA001338.

Skinner, L., and N. J. Shackleton (2005), An Atlantic lead over Pacific deep-water change across Termination I: implications for the application of the marine isotope stage stratigraphy, *Quat. Sci. Rev.*, *24*, 571–580.

Skinner, L., S. J. Fallon, C. Waelbroeck, E. Michel, and S. Barker (2010), Ventilation of the Deep Southern Ocean and Deglacial CO2 Rise, *Science*, *328*, 1147–1118.

Sortor, R. N., and D. Lund (2012), No evidence for a deglacial intermediate water Delta(14)C anomaly in the SW Atlantic, *Earth Planet. Sci. Lett.*, *310*, 65–72.

Speer, K., and E. Tziperman (1992), Rates of water mass formation in the North Atlantic ocean, *J. Phys. Oceanogr.*, *22*, 93–104.

Steffensen, J. P., et al. (2008), High-Resolution Greenland ice core data show abrupt climate change happnes in few years, *Science*, *321*, 680–684.

Stocker, T. F. (1998), The seesaw effect, *Science*, *282*, 61–61.

Stott, L. D. (2007), Comment on "Anomalous radiocarbon ages for foraminifera shells" by W. Broecker et al.: A correction to the western tropical Pacific MD9821-81 record, *Paleoceanography*, *22*, PA1211, doi:10.1029/2006PA001379.

Stott, L., and A. Timmerman (2011), The mid-depth D14C anomaly during termination 1, Do hydrothermal vents play a role?, paper presented at 11th Annual V.M. Goldschmidt Conference, Mineralogical Magazine, Prague, Chech Republic.

Stott, L., J. Southon, A. Timmerman, and A. Koutavas (2009), Radiocarbon age anomaly at intermediate water depth in the Pacific Ocean during the last deglaciation, *Paleoceanography*, *24*, PA2223, doi:10.1029/2008PA001690.

Streeter, S. S., and N. J. Shackleton (1979), Paleocirculation of the deep North Atlantic: 150,000-year record of benthic foraminifera and oxygen-18, *Science*, *203*, 168–171.

Stute, M., M. Forster, H. Frischkorn, A. Serejo, J. Clark, P. Schlosser, W. Broecker, and G. Bonani (1995), Cooling of tropical Brazil (5-degrees-C) during the last glacial maximum, *Science*, *269*, 379–383.

Talley, L. D., G. L. Pickard, W. J. Emery, and J. H. Swift (2011), *Descriptive Physical Oceanography: An Introduction*, 6th ed., 560 pp., Elsevier, Boston.

Thiagarajan, N., J. F. Adkins, and J. M. Eiler (2011), Clumped isotope calibration of modern deep sea corals and implications for vital effects, *Geochim. Cosmochim. Acta*, *75*, 4416–4425.

Thomas, A., G. M. Henderson, and L. F. Robinson (2006), Interpretation of the 231Pa/230Th paleocirculation proxy: New water-column measurements from the southwest Indian Ocean, *Earth Planet. Sci. Lett.*, *241*, 493–504.

Thornalley, D., S. Barker, W. S. Broecker, H. Elderfield, and I. McCave (2011), The Deglacial Evolution of North Atlantic Deep Convection, *Science*, *331*, 202–205.

Timmerman, A., H. Gildor, M. Schulz, and E. Tziperman (2003), Coherent Resonant Millennial-Scale Climate Oscillations Triggered by Massive Meltwater Pulses, *J. Clim.*, *16*, 2569–2585.

Toggweiler, J. R. (1999), Variation of atmospheric CO2 by ventilation of the ocean's deepest water, *Paleoceanography*, *14*, 571.

Toggweiler, J. R., J. L. Russell, and S. R. Carson (2006), Midlatitude westerlies, atmospheric CO2, and climate change during the ice ages, *Paleoceanography*, *21*, PA2005, doi:10.1029/2005PA001154.

van der Flierdt, T., L. F. Robinson, and J. F. Adkins (2010), Deep-sea coral aragonite as a recorder for the neodymium isotopic composition of seawater, *Geochim. Cosmochim. Acta*, *74*, 6014–6032.

Vidal, L., L. Labeyrie, E. Cortijo, M. Arnold, J. C. Duplessy, E. Michel, S. Becque, and T. C. E. van Weering (1997), Evidence for changes in the North Atlantic Deep Water linked to melt water surges during the Heinrich events, *Earth Planet. Sci. Lett.*, *146*, 13–27.

Waelbroeck, C., J.-C. Duplessy, E. Michel, L. Labeyrie, D. Paillard, and J. Duprat (2001), The timing of the last deglaciation in North Atlantic climate records, *Nature*, *412*, 724–727.

Waelbroeck, C., L. Labeyrie, E. Michel, J. Duplessy, J. McManus, K. Lambeck, E. Balbon, and M. Labracherie (2002), Sea-level and deep water temperature changes derived from benthic foraminifera isotopic records, *Quat. Sci. Rev.*, *21*, 295–305.

Walter, H. J., M. M. Rutgers van der Loeff, and H. Hoeltzen (1997), Enhanced scavenging of Pa-231 relative to Th-230 in the South Atlantic

south of the Polar Front: Implications for the use of the Pa-231/Th-230 ratio a paleoproductivity proxy, *Earth Planet. Sci. Lett.*, *149*, 85–100.

Wang, Y. J., H. Cheng, R. L. Edwards, Z. S. An, J. Y. Wu, C.-C. Shen, and J. A. Dorale (2001), A high-resolution absolute-dated late Pleistocene monsson record from Hulu Cave, China, *Science*, *294*, 2345–2348.

Warren, B. A. (1981), Deep circulation of the world ocean, in *Evolution of physical oceanography*, edited by B. A. Warren and C. Wunsch, pp. 6–41, MIT Press, Cambridge, Mass.

Waugh, D. W., and T. M. Hall (2002), Age of stratospheric air: Theory, observations, and models, *Rev. Geophys.*, *40*, PA2005, 10.1029/2000RG000101.

Wunsch, C. (2003), Determining pale oceanographic circulations, with emphasis on the Last Glacial Maximum, *Quat. Sci. Rev.*, *22*, 371–385.

Yu, J., and H. Elderfield (2007), Benthic foraminiferal B/Ca ratios reflect deep water carbonate saturation state, *Earth Planet. Sci. Lett.*, *258*, 73–86.

Yu, E., R. Francois, and M. Bacon (1996), Similar rates of modern and last-glacial ocean thermohaline circulation inferred from radiochemical data, *Nature*, *379*, 689–694.

Yu, J., W. S. Broecker, H. Elderfield, Z. Jin, J. McManus, and F. Zhang (2010), Loss of Carbon from the Deep Sea Since the Last Glacial Maximum, *Science*, *330*, 1084–1087.